



Facies and architecture of the Lower Messinian turbidite lobe complexes from the Laga Basin (central Apennines, Italy)

Mattia Marini^{1,*}, Salvatore Milli¹, Massimiliano Moscatelli²

¹ Dipartimento di Scienze della Terra, SAPIENZA Università di Roma, P.le Aldo Moro 5 - 00185 Roma, Italy

² CNR - IGAG, Istituto di Geologia Ambientale e Geoingegneria, Via Salaria Km 29.300 - 00016 Monterotondo Stazione, Roma, Italy

ABSTRACT - Turbidite depositional lobes are the main architectural element of many ancient turbidite systems. On modern submarine fans, they constitute sandy accumulations with lobate planform forming as terminal splays at channel mouths. Several outcrop, marine geology and experimental studies have documented how facies, depositional geometries, and overall architecture of turbidite depositional lobes can be largely controlled by the host basin morphology.

This study investigates the architecture of turbidite lobe complexes from the Southern Laga Basin (SLB; central Apennines, Italy) basing on detailed bed-by-bed correlations. During the Early Messinian, the SLB was part of a quickly deforming sector of the Apennine foreland basin system and hosted the deposition of a thick turbidite succession. The SLB's size and morphology were controlled by the balance of tectonics and sedimentation. In such a context, SLB's depositional lobes were topographically confined in an N-S trending dead-end trough delimited by thrust-related anticlines. Eventually, as turbidite sedimentation progressively smoothed out the seafloor morphology up to allow depositional lobes spilled to the E over the more external anticline..

Strike and dip sections across depositional lobes on an approximately 1700 m thick interval from the SLB's Lower Messinian, enabled us to describe and compare the depositional architecture of turbidite complexes with different degree of basin confinement.

Three main lobe sub-settings were recognized: i) a channel-lobe transition sector, where through-cross bedded and massive-to-crudely laminated beds form composite sandstone bodies which thicken down current; ii) a proximal lobe sector, where crudely laminated to planar-parallel laminated medium-fine sandstones constitute amalgamated to non amalgamated beds thinning out relatively rapidly down and across current; iii) an intermediate to distal (lobe fringe) sector characterized by deposition of thin-bedded turbidites, occasionally intercalated by debris-flow and slumping deposits.

The comparison of depositional shapes revealed the dependency of sandstone body lenticularity on thickness (and, implicitly, depositional hierarchy), lobe sub-setting and degree of topographic confinement.

At a higher hierarchical scale, the role of topographic confinement was even more important and brought about two distinctive architectures of lobe complex. Confined stratigraphic complexes show a sheet-like architecture where compensation process is unimportant and lobes gently pinch and shale out toward basin margins, whilst unconfined ones are characterized by compensational stacking of lobes and a rather intricate facies distribution.

Finally, the basin-fill scale architecture of SLB lobes was controlled by the interplay of thrusting and turbidite sedimentation, which modulated the degree of topographic confinement and caused the progressive eastward shift of the depocentre.

KEY WORDS: Turbidity currents, turbidite lobe architecture, Laga Basin, Lower Messinian.

Submitted: 16 February 2011 - Accepted: 18 March 2011

INTRODUCTION

The depositional architecture of turbidite systems hosted in structurally confined basins with active tectonics, such as those of foreland basin systems or rifted margins, strongly differs from that of present-day systems occurring along mature passive margins in front of major deltas. In these basins, topographic confinement and quickly evolving basin morphology may bring about peculiar association of sedimentary facies as well as very complex architectures in any of the architectural elements of a turbidite system. The outcrop study of well-exposed depositional analogues for such basins can provide: i) a depositional reference models for interpreting turbidite successions and hydrocarbon exploration targets hosted in similar contexts; ii) models enabling prediction of volume, geometriy and distribution of pay zones in hydrocarbon reservoirs and; iii) a conceptual

framework and useful statistical parameters for stochastically modelling petrophysical properties in turbidites.

Physical stratigraphy, facies analysis (Milli et al., 2007; Falcini et al., 2009; Marini, 2010) and basin analysis (Bigi et al., 2009) studies carried out in recent years on the Messinian Laga Basin, have already outlined the depositional architecture of its turbidite infill, as well as the timing of tectonic deformation and basin morphology modification.

The work detailed here will deal with the Lower Messinian depositional lobes from the Southern Laga Basin (SLB) and its aim was twofold. The first aim was to evaluate the influence of topographic confinement on the depositional architecture of turbidite lobes by comparing facies spatial distribution, sandbody geometries and staking patterns from different stratigraphic intervals. The second aim was to provide a depositional analogue for turbidite lobes hosted in confined basins with active tectonics.

*Corresponding author: mattia.marini@uniroma1.it

Depositional lobes in modern fans and turbidite systems: a short review

The term lobe does not have the same connotation for modern submarine fans as it does for ancient turbidite systems (Mutti and Normark, 1987). This is because most of the studied lobes from modern fans have been generally described mainly basing on their morphology whilst few are the data on sedimentary facies and internal architecture. This makes hierarchical scale and origin of present-day lobes hard to infer and does not enable a straightforward comparison with sandstone lobes from ancient turbidite systems.

On modern fan, depositional lobes constitute positive features of seafloor topography with lobate planform occurring down-stream of canyons and channels, whose size, lifetime and, implicitly, hierarchy may change within a quite broad range (Mutti and Normark, 1987, 1991).

In ancient turbidite systems, sandstone lobes were first recognized in 70's (Mutti and Ghibaudo, 1972) and described as non-channelized, prograding bodies, ranging in thickness from few m to some tens of m, composed of thick-bedded sandstone alternating with thinner bedded and finer-grained interlobe facies. Divergent paleocurrent directions were early (Mutti and Ricci Lucchi, 1972) recognized as a proof for lobate planform and, as such, accounted as one of the most typical facet of lobe sandstone bodies.

The association of non-channelized sandstone bodies and channelized facies brought to light by outcrop studies in the late 70' was reconciled with the original definition of sandstone lobes by the model of Mutti (1979). In this model, sheet-like, tabular sandstone bodies characterize the flat outer region of mixed-sediment, highly efficient systems, whilst the association of channelized and non-channelized sandstone bodies makes up channel-attached lobes of sand-rich, poorly efficient systems.

Thickening-upward sequences, recognized by Mutti and Ghibaudo (1972) and Mutti and Ricci Lucchi (1972) as an evidence of the prograding nature of depositional lobes, were later on interpreted by Mutti and Sonnino (1981) as compensation cycles originating from deposition of successive lobes in topographic lows.

The prograding nature of depositional lobes was also disputed by Hiscott (1981) basing on the fact that asymmetric cycles (i.e. facies sequences) are not universally recognized and that gradual channel abandonment as envisaged in the feeding systems of lobes, should result in the preponderance of thinning-upward sequences in lobe deposits. In a reply to this discussion, Ghibaudo (1981) stressed that only fine-grained systems with extensive lobes that gradually shale out into the enclosing fan fringe and basin plain are likely to develop thickening-upward sequences as the whole system progrades out into the basin. On the contrary, sand-rich fans are characterized by small coarse-grained lobes that wedge-out abruptly into the surrounding basin plain and give rise to random rather than clear progradational sequences.

Where turbidity currents are not obstructed by topography, the 3D geometry and internal architecture of turbidite depositional lobes mostly depends on flow dynamics outboard of canyons and channel mouths. Tanks experiments showed that, similarly to what has been observed on modern submarine fans, a lobate planform characterizes the deposit of unobstructed flows (Luthi, 1981; Kneller, 1995).

Disregarding the basin-scale effect of topographic confinement, bathymetric data from modern fans show how

the transition from channels to depositional lobes coincides with a major gradient break in the along-dip section of present-day turbidite systems, across which turbidity currents switch from an accumulative, waxing behaviour to a depletive, waning behaviour loosing competence and capacity. This change in flow behaviour is also favoured by flow expansion and sudden dilution occurring at channel mouth, and marks the hinge point between a sector where erosion and deposition alternate in time and a sector where net-deposition occurs.

Recent studies from both modern fans (Gervais et al., 2006; Deptuck et al., 2008) and ancient turbidite systems (Sinclair, 1994; Amy et al., 2007; Satur, 2000) suggest that lobe architecture and sedimentary facies types and distribution may be strongly controlled by topographic confinement. This is also confirmed by experimental studies which have since long demonstrated the role of topographic obstacles and confining topography on deposit geometry and character (Al-Ja'aidi et al., 2004; Amy et al., 2004).

In the modern sand-rich Golo System (eastern margin of Corsica, Tyrrhenian Sea), lobe architecture is primarily controlled by depocentre morphology and is characterized by compensational stacking of successive stages of growth (Gervais et al., 2006). Comparison of high-resolution seismic data of lobes from other modern systems off the eastern margin of northern Corsica (Deptuck et al., 2008) showed that seafloor slope and basin morphology is one of the main control factors for lobe planform whilst internal architecture is mainly related to lobe lifespan (and, implicitly, hierarchy) and feeder channel geometry and stability. Moreover, the Lobe thickness/width ratio calculated by (Deptuck et al., 2008) indicates a positive correlation between the two geometric parameters and a higher lenticularity of lobes in their proximal sectors.

GEOLOGICAL AND STRATIGRAPHIC SETTING

The central Apennines are part of a fold-and-thrust belt built up since the Late Oligocene in response to the subduction of the Adria micro-plate (i.e. a promontory of the Africa Plate) underneath the European Plate (Patacca et al., 1990; Carminati et al., 2004).

Progressive tectonic accretion and loading of subducting lithosphere in the Appenine subduction complex (Doglioni, 1991) resulted in the development of a highly articulated foreland basin system, filled up by relatively thick, diachronous turbidite successions (Ricci Lucchi, 1986). From W to E, these are the Macigno Fm. (Chattian-Burdigalian), the Cervarola Fm. (Burdigalian-Langhian), and the Marnoso-arenacea Fm. (Langhian-Lower Messinian).

From the Late Tortonian onwards, the physiography of the Apennine foreland basin system changed in response to an intense tectonic activity that lead to the fragmentation of Marnoso-arenacea Basin into smaller, elongated turbidite basins delimited by thrust-related anticlines (Centamore et al., 1978).

During the Messinian, the Laga Basin was the largest and easternmost (i.e. most external) of these basins and hosted the deposition of a thick turbidite succession (namely, the Laga Fm.) whose architecture, in turn, records the progressive depocentre-shift to the Pliocene-to-Present foreland basin system (Milli et al., 2007). The basin extended for approximately 120 km in an SE-NW direction and was dissected by a WSW-ENE fault (Fiastrone-Fiastrella fault, Cantalamessa et al., 1980, 1983, 1986; Calamita et al., 1994) in

a northern relatively stable sector (the Northern Laga Basin, NLB), and a southern subsiding depozone, namely the Southern Laga Basin (SLB).

At present, the SLB is bounded by three regional thrusts which from the E to the W and the lower to the higher in the structural edifice are the Teramo thrust (T1), the Gran Sasso thrust (T2) and the Sibillini thrust (T3) (Fig. 1).

T1 superimposes the Laga Fm. onto the younger turbidites of the Cellino Fm. Its pre-Late Messinian activation is infearable (Bigi et al., 2009) from its throw, which progressively decreases at shallow levels.

T2 and T3 superimpose the meso-cenozoic slope-to-basin calcareous-marly successions onto the Laga Fm. Both of these thrusts were active all along the Messinian and controlled the position of the inner slope and the southern basin margin, respectively (Milli et al., 2007; Bigi et al., 2009, 2011). The geometrical relationship between the Lower Messinian turbidites and the pre-turbidite substratum from basin-scale correlations (Milli et al., 2007) would indicate a Early Messinian activation of T2.

Within the SLB, the structural style is characterized two N-S trending thrusts, namely the Acquasanta thrust and the Montagna dei Fiori-Montagnone thrust. The total shortening associated to these thrusts is relatively small (approximately 12% along an E-W transect across the study area of Fig. 4) and mainly occurs at depth (Bigi et al., 2009) suggesting that the outcrop area of the Laga Fm. roughly coincides with the maximum extent of the turbidite basin in the Messinian.

The shortening associated to the Acquasanta thrust

rapidly decreases toward the S where, also, its hangingwall anticline plunges and broadens into the open fold along the Mt. Gorzano western flank. A late-Early Messinian activation of the Acquasanta thrust has been inferred from the sudden change in paleocurrents, which in the upper-Lower Messinian beds are redirected to the S (Milli et al., 2007; Bigi et al., 2009), that is, parallel to Acquasanta anticline trend.

Although the age of activation of the Montagna dei Fiori-Montagnone thrust is debated, the onlap of the Lower Messinian turbidites onto its hangingwall anticline (Casnedi et al., 2006) would suggest an Early Messinian deformation. In this interpretation, the culmination of the Montagna dei Fiori-Montagnone Anticline bounded the turbidite basin to the E until it was buried by turbidite sedimentation.

The Upper Tortonian-Lower Pliocene Laga Fm. turbidites crop out in Southern Marche and Abruzzi and have been recently subdivided into three allostratigraphic units (from the older to the younger, Laga 1, Laga 2 and Laga 3) whose age as been inferred by correlating their bounding unconformities (I1, I2 and I3 in Fig. 2; Milli et al., 2007) to the Messinian events recorded elsewhere in the Northern Apennine (Roveri et al., 1998; Rossi et al., 2002; Artoni, 2003, 2007; Manzi et al., 2005).

The Laga 1 and Laga 2 units (pre-evaporitic stage, 7.251-5.96 Ma and Evaporitic stage, 5.96-5.6 Ma, respectively) crop out extensively in the footwall of the Sibillini Mts. thrust and progressively thin to the E onlapping the western limb of the Montagna dei Fiori-Montagnone Anticline (Fig. 1). In the footwall of the Acquasanta thrust, the Laga 1 and Laga 2

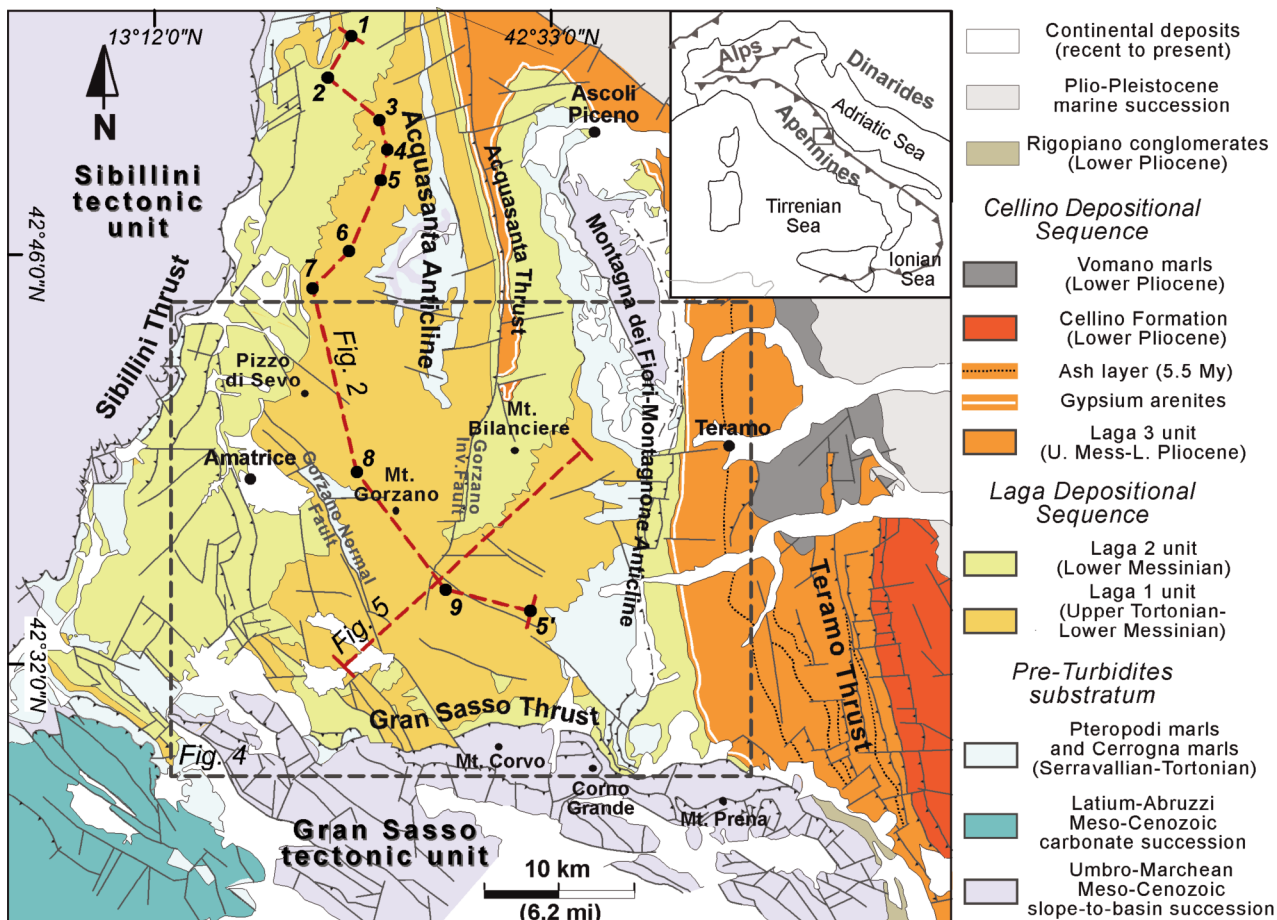


Fig. 1 - Simplified geological map of the Southern Laga Basin. Modified after Centamore et al. (1991).

units are present in the subsurface and pinch out to the E, whilst the Laga 3 (Late Evaporitic stage, 5.6-5.1 Ma) crops out extensively with a maximum thickness of about 3000 m.

The Laga Fm. and the younger Cellino Fm. turbidites (Fig. 1) have been also interpreted as part of two 3rd-order depositional sequences stacked in an overall progradational pattern for the E-ward depocentre-shift induced by thrusting (Milli et al., 2007).

The older of these sequences, namely the Laga Depositional Sequence (LDS), comprises the Laga 1 and Laga 2 alluviums and is the object of this work. LDS is separated by the younger Cellino Depositional Sequence (CDS) by a regional unconformity related to the infra-Messinian regional tectonic event (Milli et al., 2007).

CDS comprises the Laga 3 unit (Late Messinian), the Marne del Vomano Fm. (Early Pliocene) and the Cellino Fm. (Early Pliocene, Fig. 1) and records the onset of Late Messinian-to-Present foreland basin system.

The Laga Depositional Sequence (LDS)

Sedimentology and basin analysis studies (Milli et al., 2007; Bigi et al., 2009, 2011) have recently outlined the gross depositional architecture of LDS as well as facies associations characterizing the elements of its turbidite systems.

In a stream-wise direction, from NW to SE, three main architectural elements have been described (Fig. 3): i) a main proximal, channelized sector; ii) an intermediate channel-lobe transition sector; iii) a distal, lobe sector.

The main channelized sector occupied the northern part of the basin extending to the south for about 20 km (sections 1-8 in Fig. 2) and was constituted by a belt of braided channels topographically constrained by the inner slope to the W and by the base of the foreland ramp to the E. Steeper and smaller channelized complexes were also present all along the inner slope and probably fed by a number of canyons and slope-channels (e.g. Isola San Biagio sector, see Milli et al., 2007) cut in the pre-turbidite substratum along T3 tear faults associated to T3. Channelized deposits are constituted by very thick-bedded, sandstone bodies with mud-draped basal scours internally showing fining up-ward facies sequences with coarse-grained trough-cross stratified sandstones passing up-ward to unchannelized, massive to ripple-laminated sandstones.

The channel-lobe transition sector is not easily definable as its deposits are an association of channelized to unchannelized sandstones ubiquitous either in the channel sector or proximal depositional lobes. It may have essentially represented an along-stream segment of turbidite systems where, due to a significant gradient break, channels gradually widened in response to gradual loss of momentum and erosive ability by turbidity currents.

Finally, downstream of channels mouths, the lobe sector was represented by a relatively small basin plain morphologically confined by thrust-induced topography.

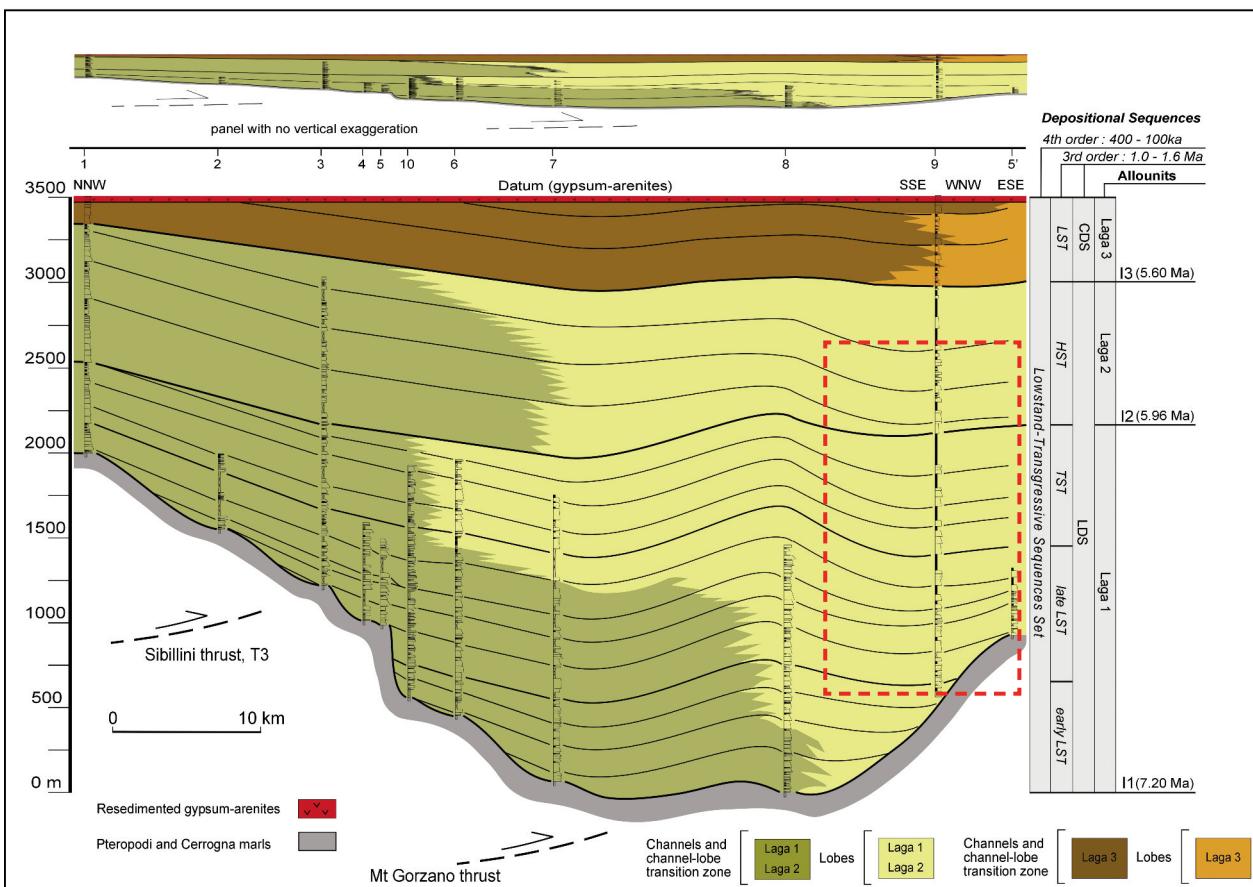


Fig. 2 - Dip-section of the Laga Basin turbidite infill (for its location see Fig. 1). Mean palaeoflow direction is toward the right. The red dashed rectangle show the stratigraphic and geographic position of the studied interval. Note the turbidite lobes of the Laga 1 Unit onlapping the Gran Sasso frontal ramp between sections 8 and 9. Modified after Milli et al. (2007, 2009).

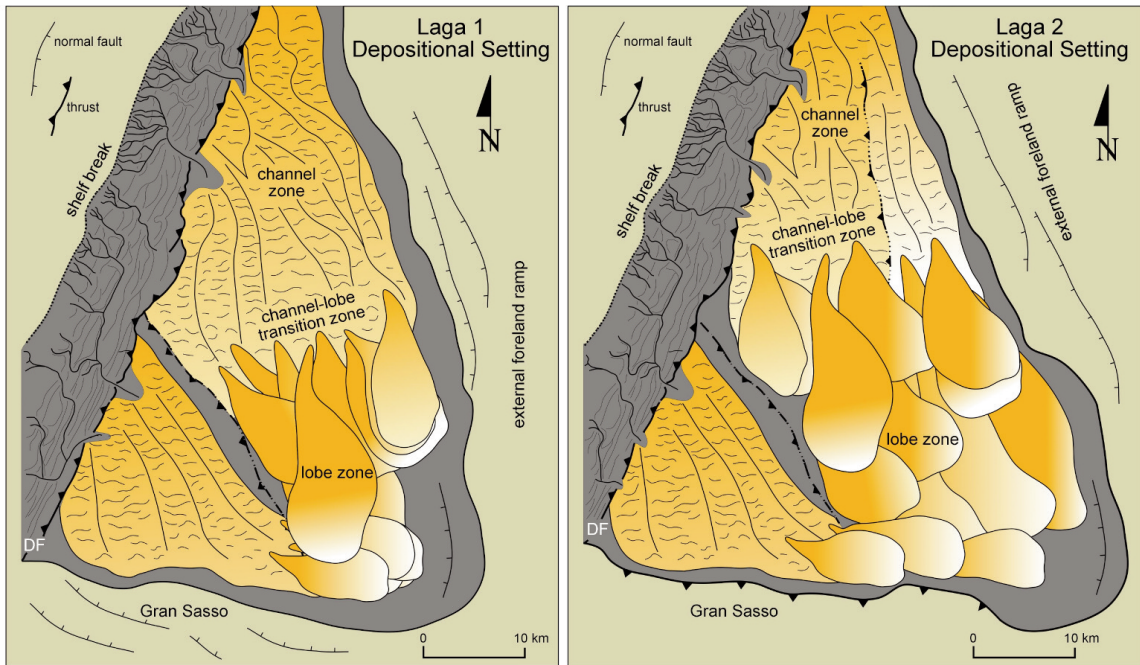


Fig. 3 - Simplified sketch showing the physiography of the Laga 1 and Laga 2 turbidite systems.

STUDY AREA

The study area (Fig. 4) is located in the southeastern part of the Laga Basin and extends from the Campotosto Lake to the Montagna dei Fiori-Montagnone Anticline and from the southernmost reach of the Acquasanta Anticline to the foothill of the Gran Sasso Range. The major tectonic features dissecting this area are the SW-dipping Mt. Gorzano. Normal Fault, which exposes the boundary between the Laga Fm. and the pre-turbidite substratum, and the Gorzano Mt. inverse fault, which represents the southernmost expression of the Acquasanta thrust. Both of these structures roughly trend N-S. To the E of the Gorzano Mt. Normal Fault, the whole thickness of Laga 1 and Laga 2 units and the lowermost part of the Laga 3 unit crop out extensively, whilst to the W, only the Laga 1 unit crops out, albeit strongly deformed by a network of minor faults (Fig. 5).

The succession exposed in study area has been object of study since the late70' (Mutti et al., 1978; Morelli, 1994; Corda and Morelli, 1996; Casnedi et al., 2006) and so far referred to an outer fan setting (*sensu* Mutti and Ricci Lucchi, 1972, 1975). More recently, other workers (Milli et al., 2007; Marini et al., 2009; Marini, 2010) showed how, at least during the Early Messinian, depositional lobes might have been contained in a relatively small basin plain, topographically confined by growing anticlines.

METHODOLOGIES AND DATASET

To do this work 27 stratigraphic-sedimentological sections were measured in the field (Fig. 4) from the upper part of the Laga 1 unit and the lower part of the Laga 2 unit covering a 1700 m-thick stratigraphic interval of turbidite lobe deposits. Sections were logged in detail describing all the relevant bed physical features (base and top characteristics, internal structure, grain size, bed geometry, etc.) and key beds walked out in the field to establish a robust correlation framework.

The general correlation panel (Fig. 5) obtained correlating

most of the measured sections is roughly perpendicular to the mean palaeoflow direction and extends from the Campotosto Lake to the western limb of the Montagnone Anticline.

The best-exposed stratigraphic intervals from the studied lobe complexes were chosen for carrying out bed-by-bed correlations and comparing the architecture of distinct lobe sub-setting developed under deferent degree of topographic confinement. To make this comparison more objective and quantitative, facies statistics were computed for units of comparable hierarchy (Figs. 17 and 20), which roughly coincides with the 4th turbidite sub-stages of Mutti and Normark (1987), and sandstone body thicknesses plotted against distance from a reference point along their profile (Fig. 21).

FACIES AND DEPOSITIONAL PROCESSES

Facies analysis allowed defining six main facies that will be hereby described and interpreted basing on their spatial and genetic relationship.

Facies L1

L1 is represented by trough-cross-stratified (Fig. 6a), coarse to medium-grained sandstones forming thick to very thick amalgamated beds. In the along-paleoflow direction, L1 shows foresets with low-angle to nearly tangential basal contact (Fig. 6b). L1 may either overlie or underlie massive to laminated sandstones (Facies L2) or be closed at its top by a sharp, by-pass surface on top of which sandstones with ripple-drift cross lamination (Facies L4) or mudstones (Facies L5) can occur. L1 passes to Facies L2 both laterally and down-current.

L1 is common in the lower LDS from the western sector of the SLB where it forms lenticular sandstone bodies with scoured base, which thicken down-current.

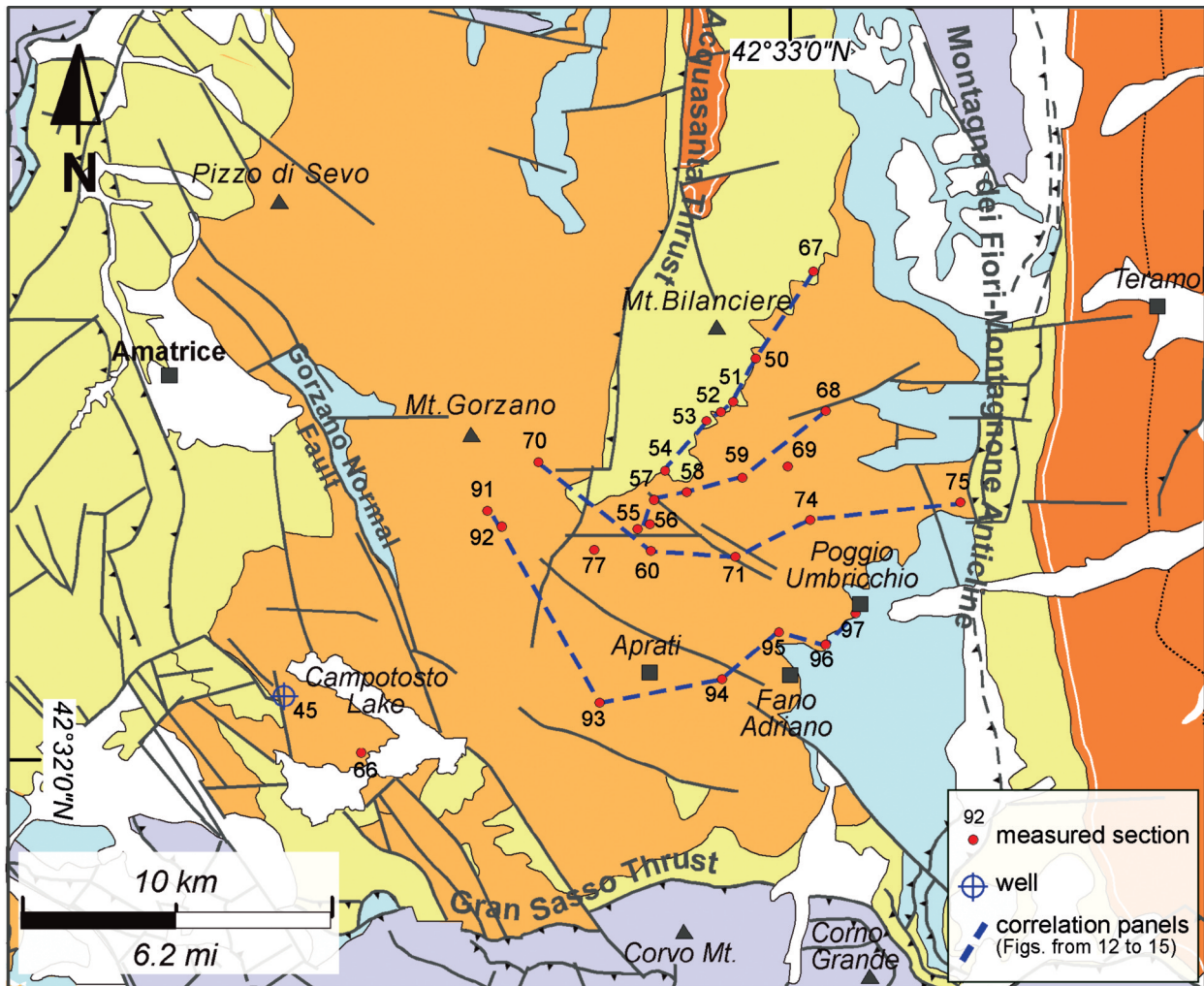


Fig. 4 - Simplified geological map of the study area showing the location of stratigraphic-sedimentological sections and correlation panels presented in the following paragraphs.

Inferred depositional processes and interpretation of Facies L1

These trough-cross stratified sandstones represent stacks of medium to large, flat (i.e. low amplitude, large wavelength), 3D dunes (sensu Ashley, 1990). The low-angle-to-tangential basal contact of lee sides is probably due to flow separation at the bedform crest and reverse flow in the trough, and may indicate a relatively high flow velocity. These features, together with mean grain size, depositional geometries and spatial occurrence of this facies suggest deposition in a channel-lobe transition setting where turbidity currents deposited the coarsest sediment fraction and organized it in bedforms while by-passing the bulk of their sedimentary load farther down-current.

Facies L2

L2 is constituted by massive-to-crudely laminated and planar-parallel laminated medium-fine grained sandstones. Normal distribution grading is frequent, whilst the coarsest fraction, may occasionally give rise to coarse-tail normal grading at the very base of L2 beds.

In this facies, poorly developed, laterally discontinuous and non-parallel laminae represent a continuum from massive,

dewatered sandstones to crudely laminated sandstones, and may grade upward into a planar-parallel laminated interval (Fig. 7).

In planar-parallel laminated intervals, individual lamina may reach a thickness of 2-3 cm and show either normal or inverse grading with either a coarser grained, brighter layer grading upward into a finer grained, darker layer, or viceversa.

Dewatering gives rise to dish and pillar structures in the lower part and deformation of pre-existing laminations in the upper part of L2 beds.

At the base of L2 beds, mudstone and sandstone rip-up clasts and large rafts (up to some dm) may be present and locally imbricated. Conversely, rounded cm mud chips are more frequent in the upper part of L2 beds.

The base of L2 beds is always sharp and locally slightly erosive with sole casts (i.e. flute, groove, and frondescent casts) or erosive with tabular scours. Loading deformation in a "ball-and-pillow" fashion may be present at the base of L2 beds when they rest on top of mudstones.

L2 generally gives rise to thin to thick event beds, which in turn may be amalgamated in very thick beds and mega beds.

In sand-rich intervals, L2 may account for up to 75% of total sandstone thickness, is found laterally and/or down current of L1 and may transitionally grade upward into ripple-drift laminated sandstones of Facies L4. Sharp passage to either L4

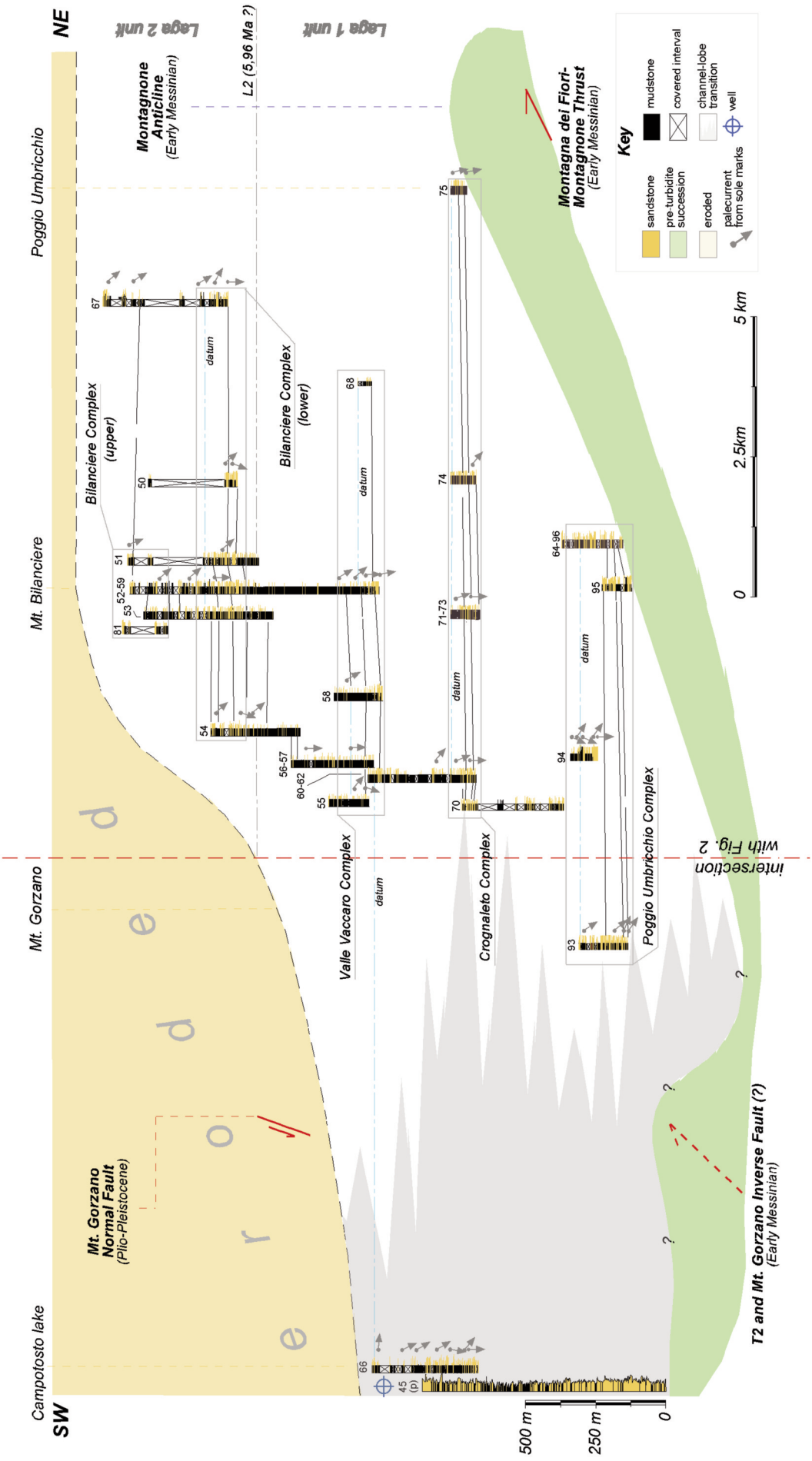


Fig. 5 - Correlation panel through the LDS turbidite lobes from the Southern Laga Basin. Mean palaeoflow direction is toward the viewer.

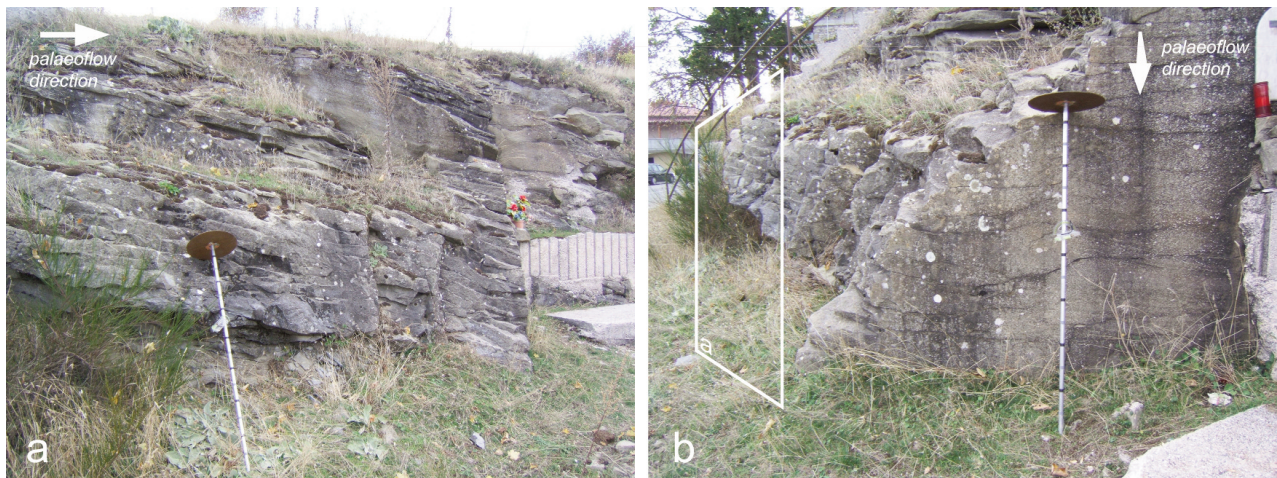


Fig. 6 - Dip section (a) and strike section (b) of Facies L1 showing forests and trough-cross stratification, respectively. Jacob's staff is 1.5m.

or mudstones (Facies L5) is generally marked by mm's-thick lags of phytoclasts.

L2 is amply described and discussed in the literature and commonly referred to as Ta-Tb Bouma divisions (Bouma, 1962) and F8 of Mutti (1992).

Inferred depositional processes and interpretation of Facies L2

This facies is interpreted as the product of a quickly aggrading, relatively high-concentrated basal layer of a turbulent flow. As function of the ratio between rate of sedimentation from above and shear exerted at the water-sediment interface, traction may have been totally or partially suppressed, resulting in deposition of massive-to-crudely laminated sandstones, or may have given rise to well-developed planar-parallel lamination. Upward migration of water trapped in the fast-settled basal part of L2 beds and local fluidification are responsible for escape structures and

large-scale deformations. Small and tabular erosive features found at the base of L2 beds and rip-up clasts and rafts would suggest some erosive ability of parent flows.

Facies L3

L3 is constituted by structureless, poorly sorted muddy sandstones rich in mudclasts. Matrix mud is not uniformly distributed in L3 beds and blebs with irregular shape of cleaner sands may be present at different heights from the base. Cm's to dm's, sub-horizontal lying rip-up mudclasts are abundant in L3 lower half and are replaced upward by smaller and better rounded mud chips. On some outcrops rip-up clasts at the very base of L3 beds are still attached to the underlying mudstone beds from which they originate and the encasing sandstone is relatively mud-poor.

Phytoclasts are often present and locally abundant. They are generally homogenously distributed and either sub-horizontal or randomly oriented, although may be concentrated to form small pockets with irregular ameboidal shapes.

L3 forms beds rarely thicker than few tens of cm and overlies either L2, ripple-drift laminated sandstones (Facies L4) or mudstones (Facies L5) on top of sharp, slightly erosive surfaces (Fig. 8). It may transitionally pass upward to or be capped by L4 or L5.

L3 is present throughout the studied interval but mainly occurs within shaly, heterolithic intervals separating thick sandstone lobes. In sand-rich intervals, L3 is found laterally to L2 and L4 at basin margins (Figs. 16 and 17) or on flanks of sandy depositional bulges (Figs. 18 and 19) where it is relatively cleaner (i.e. contains smaller percentage of matrix-mud) and bears higher concentrations of large rip-up mudstone clasts.

This facies has been described by many Authors from a number of turbidite basins and referred to as "slurried" bed by early workers (Ricci Lucchi, 1978, 1981; Mutti et al., 1978; Ricci Lucchi and Valmori, 1980; Muzzi Magalhaes and Tinterri, 2010), slurry flow deposit (Lowe and Guy, 2000; Lowe et al., 2003; Sylvester and Lowe, 2004) and, more recently, as debrite (Talling et al., 2004; Haughton et al., 2003, 2009; Davis et al., 2009).



Fig. 7 - Event bed of Facies L2 with a basal massive-crudely laminated interval (below the compass) passing upward to a relatively thick interval with planar-parallel lamination.



Fig. 8 - Muddy sandstones of facies L3 bearing large, sub-horizontal laying mudstone rafts sit on top of an amalgamation surface.

Inferred depositional processes and interpretation of Facies L3

The most remarkable feature of Facies L3 is its poor sorting and relatively high content in matrix-mud and mudclasts. The abundance of matrix-mud strikes with a process of settling from a turbulent low-density suspension, which would have yielded a better sorting to this facies. Similarly, distribution and arrangement of phytoclasts and mudclasts, whose hydrodynamic behaviour is expectedly different from that of sand grains, suggest that the load might have been deposited as a whole rather than settled layer by layer. Nonetheless, the banding of some beds or arrangement of phytoclasts, would exclude an *en masse* deposition as well as a major role by traction, which might have winnowed away the mud-grade fraction.

The large sub-horizontal rip-up clasts present at the base of L3, which are in some instances still attached to beds from which they were torn away, indicate that the flow might have been able either to rip-up mudstone clasts or entrain mud-grade particles from non-consolidated sediments. Replacing of rip-up mudclasts by rounded mud chips in the upper half of L3 beds can be explained by a process of abrasion and down-sizing of clasts in a near-bed shear layer (see Lowe and Guy, 2000). Finally, near-bed shear and late-depositional stage deformation may be also accounted as possible causes for the banded appearance of some L3 beds and formation of clean-sand blebs through a process of localized mud elutriation (cf. stress pillars of Lowe, 1975).

These features altogether are consistent with deposition by a cohesive-laminar flow (i.e. a debris flow in the definition of Postma, 1986) originating from decelerating, small volume turbidity currents. The small volume of L3 parent flows can be inferred from the typical thickness of L3 beds. Flow transformation from a fully turbulent flow into a cohesive debris flow may have taken place for progressive dampening of turbulence as the mud content in the flow increases *en route* up to reach a critical concentration. Above such a concentration, gelling of clay minerals might have resulted in strong, interlocking cohesive forces able to fully suppress turbulence and force the mud-sand mixture (i.e. slurry) to move down current as a cohesive laminar flow (Baas et al., 2009). In such a process, flow interaction with a non-firm seafloor and topography may have greatly contributed to enhance mud entrainment and force the flow to decelerate

over short distances, well before the newly entrained mud could be elutriated.

Facies L4

Facies L4 (L4 hereafter) is represented by muddy very fine sandstones with ripple-drift cross to sinusoidal lamination or convoluted lamination passing upward to planar-parallel laminated siltstones and clayey siltstones. The base of L4 beds is always sharp and may present small groove and flute casts.

L4 is generally interbedded to mudstones (Facies L5) into which may grade upward and may transitionally overlie either L2 or L3. On some outcrops, L4 beds with convoluted laminae and deformed bedding surfaces pass laterally to structureless muddy sandstones of Facies L6.

L4 is widespread throughout the studied interval but volumetrically significant in mud-prone intervals and in heterolithic units only. It is amply described and discussed in the literature and commonly referred to as Tc-Td Bouma divisions.

Inferred depositional processes and interpretation of Facies L4

This facies is the product of traction-fallout processes in low-density waning-depletive turbidity currents (sensu Kneller, 1995). Late-to-post depositional soft-sediment deformations favoured by overpressured water are responsible for convoluted lamination (Sanders, 1965) and, on thicker beds, to fluidification and full homogenization of the deposit.

Facies L5

Facies L5 (L5 hereafter) is represented by interbedded, laminated to structureless mudstones intercalated by TBT. Laminated mudstones are often rich in horizontal-lying phytoclasts and form thin beds with lighter grey hue while massive mudstones generally constitute very thick caps to sandstone lobes.

On few outcrops from the Laga 1 unit (Poggio Umbricchio and Crognaleto Lobe complexes, see next paragraphs), thick L5 beds are dissected by m-scale, tabular to ptygmatic sand injections, with thickness ranging from few mm to few cm (Fig. 9).

Inferred depositional processes and interpretation of Facies L5

L5 Facies is the product of fall-out from very dilute turbidite clouds and, probably, haemipelagic sedimentation. The planar-parallel lamination characterizing siltstones and iso-oriented fitoclasts suggest traction at the water-sediment interface whilst structureless mudstones may be explained by a relatively quick deposition for flocculation of clay minerals possibly promoted by ponding of turbidity currents.

Generation of fractures and sand injection would result from fracturing of consolidated, quasi-brittle behaving mud and sand-advection by up-ward migrating water. As in polygonal faulting, fracturing may have been induced by volumetric contraction related to compactional dewatering, gravitational instability due to density inversion (and associated dewatering) and to gravitational spreading/sliding (Watterson et al., 2000).

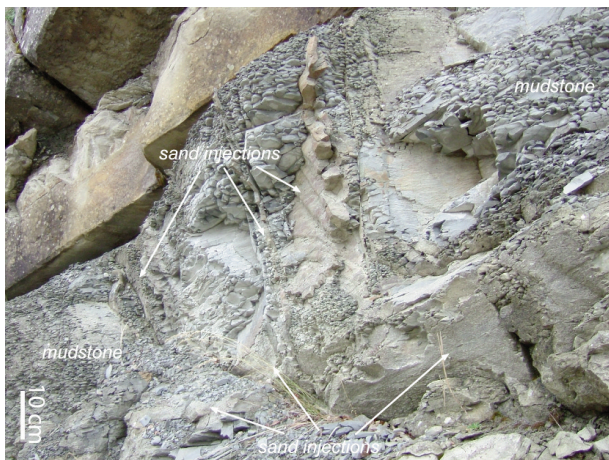


Fig. 9 - Facies L5. Sand-injected mudstones.

Facies L6

Facies L6 comprises a range of deposits from slumped packages to either chaotic or structureless muddy sandstones.

Slumped packages (Fig. 10a) of L6 are constituted by m-thick heterolithic intervals of thin-bedded turbidites from slightly-to-strongly deformed showing on the outcrop face open to recumbent folds. These packages are commonly either dissected by joints and faults or injected by small sandstone sills and dikes. Sand injections (II in Fig. 10a) show a variety of shapes from irregular-cauliform, to planar and ptygmatic and are fed from inside the outcrop face or from below by muddy sandstones (L3) beds, which consistently

underlie L6 with sharp, deformed contacts.

Because of their emplacement mechanism, tops of these slumped packages are generally hummocky with topographic lows filled in by chaotic deposits (I in Fig. 10). These are represented by a matrix of muddy sandstone encasing folded sandstone and mudstone rafts and are followed upward by L5 and L4 thin beds, which eventually suture the microtopography of the slump top (Fig. 10).

Chaotic deposits can also occur separately, laterally to slumped packages, and internally show folds, sub-horizontal shear planes and sandstone/mudstone rafts aligned along low-angle shear bands.

To L6 are also referred some structureless muddy sandstones resembling those of L3 but lacking mudstone rip-up clasts. These dirty sandstones pass laterally to strongly deformed L4 beds with either ripple-drift cross-lamination or convolute lamination (Fig. 10b).

The suite of deposits grouped in this facies show similarities with either slumps (Muzzi Magalhaes and Tinterri, 2010) or some debrites (see Figs. from 5 to 8 in Haughton et al., 2003).

Inferred depositional processes and interpretation of Facies L6

As the different typologies of deposits ascribed here to L6 are intimately associated spatially, any genetic interpretation must satisfactorily explain a variety of processes from slumping of non-consolidated sediments, to injection of liquefied sands and emplacement of chaotic/structureless muddy sandstones.

Slumped heterolithic packages consistently sit on top of

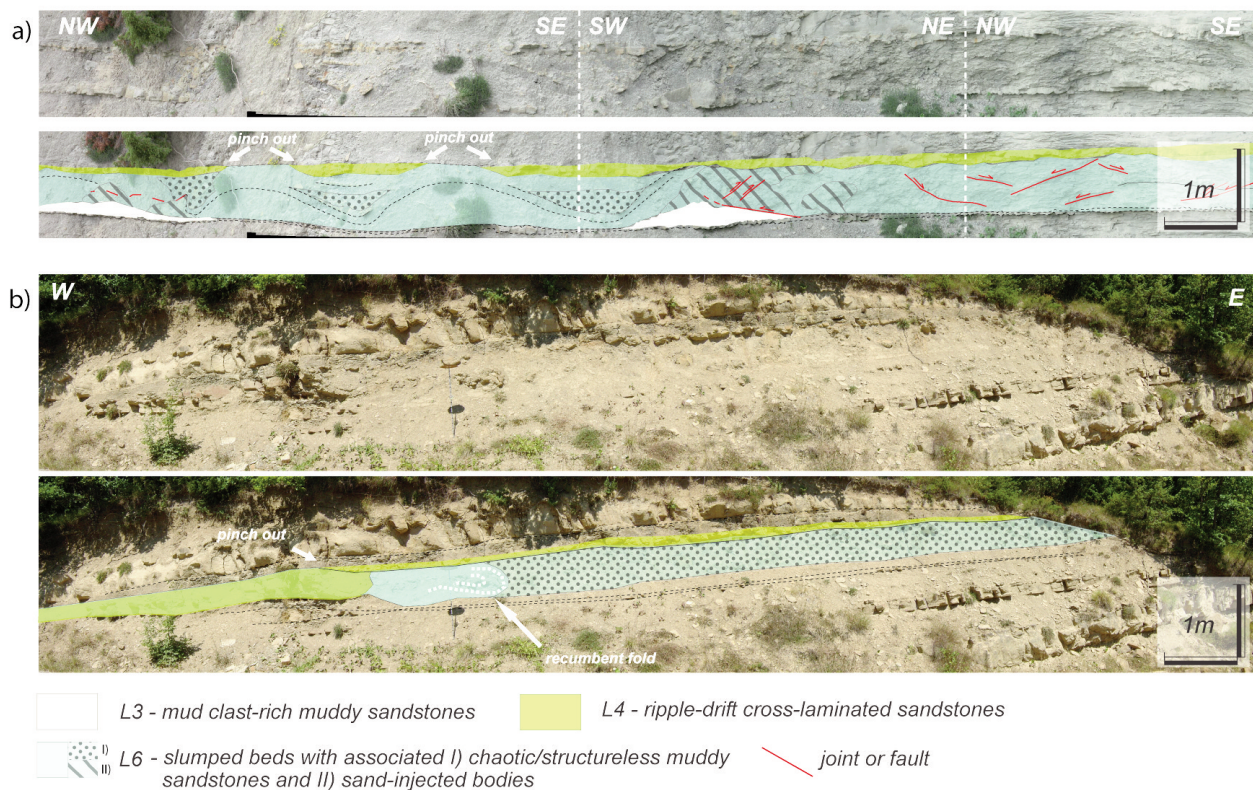


Fig. 10 - Slumps and soft-sediment deformations in Facies L6. In (a) a slumped TBT package sits on top of mud-clast rich muddy sandstones (facies L3, see text for its description), which behaves as decollement horizon and is squeezed out beneath antiforms to source fluidized sands to injected bodies. Chaotic muddy sandstones fill in the topographic lows (at the core of synforms) of the package top surface. In (b) a relatively thick bed of ripple-drift cross-laminated sandstones is deformed in a recumbent fold and passes laterally to structureless muddy sandstones.

L3 with a sharp irregular contact often pierced by sand injections. Given its content in matrix mud, mud calsts and phytoclasts, L3 might have yielded very poor geotechnical properties (i.e. a relatively low shear strength) making it a good candidate as décollement level for slumping. Furthermore, especially were overlaid by mudstones, consolidation of L3 might have been a very slow process favouring the bulding up of porewater pressure for loading by successive beds. Initiation of sliding over the basal décollement may have been penecontemporaneus to fluidization and upward injection of L3 sands. The overall rheology of slumped units may have been plastic mainly owing to the cohesive behaviour of mudstones, which embodyng sand layers prevented sand and mud beds to mingle. At the top of slumped units, chaotic muddy sands may represent the product of gravitational instability of loose sediments.

Chaotic units not overlying slumped packages may have been deposited by debris flows originating downslope transFm. of slumps. Finally, muddy very fine sandstones may be interpreted as the product of either deposition by a debris flow with long run-out distances or in loco homogenization of unconsolidated ripple-drift laminated muddy sands (Facies L4) caused by liquefaction. In the former case, run-out distance may have been sufficiently long for efficiently mixing the sediments involved, but have not promoted a significant water entrainment and dilution.

Seismic shocks, shear by overriding turbidity currents or overloading by successive turbidite beds may be all regarded as causes for initiation of processes and flow types originating L6.

DEPOSITIONAL ARCHITECTURE

Four hierarchical orders (Fig. 11) have been defined from event beds to lobe complexes, basing on thickness thicknesses and internal organisation of depositional bodies. Bed thickness classification refers to that of Campbell (1967).

Very thin to thick beds, which in the studied succession are generally thinner than 1 m, are mostly devoid of internal amalgamation surfaces and could be interpreted as the product of single depositional events by turbidity currents. Such beds, here called event beds, and their depositional meaning recall the definition of bed of Campbell (1967). The

term event bed in place of bed is here preferred since it better indicates the almost instantaneous nature of the deposition event. Although it could be questioned that all of the sandstone bodies whose thickness does not exceed 1m must be considered the product of single depositional events by turbidity currents, to the purpose of this hierarchical classification such generalization seems reasonably acceptable.

Thick to very thick sandstone beds internally show several amalgamation surfaces, which separate thinner event beds and are marked either by mudstone clasts alignments or sharp breaks in grain size, which separate thinner event beds and. By their nature, these composite beds must be interpreted as the product of deposition by several flows and constitute units 10 to 15m thick here called lobe stacks. It should be noted that the character (thickness, 3D geometry, facies sequences, sand/mud ratio etc.) of lobe stacks strongly vary from proximal to distal lobes. In distal to lobe-fringe settings, lobe stacks may be represented by relatively thin heterolithic packages. Lobe stacks generally show a coarsening-thickening upward trend in their lower part turning into a clearer opposite trend in their upper part. Such internal organisation would reflect high-frequency variation in sediment delivery to depositional lobes possibly related to climate.

Sedimentary successions comprising several lobe stacks are here called lobe sets. Lobe sets are few tens of m thick and show a coarsening-thickening upward trend in their lower portion, which turns into a fining-thinning upward trend in their upper part. The architecture of lobe sets can be controlled by autocyclic processes such as compensation of depositional topography and channel avulsion in up-dip sectors, or allocyclic factors such as climate and inland drainage pattern evolution.

At a larger scale, a lobe complex is a sedimentary succession few hundreds of m thick, made up of several lobe sets. Lobe complexes too, show an overall coarsening-thickening upward trend in their lower part and an opposite trend in their upper part. Although the internal organisation of a lobe complex is largely controlled by the architecture of its building blocks, tectonics can play a major role on its overall geometry and pattern of sand distribution for example by controlling the basin size and morphology.

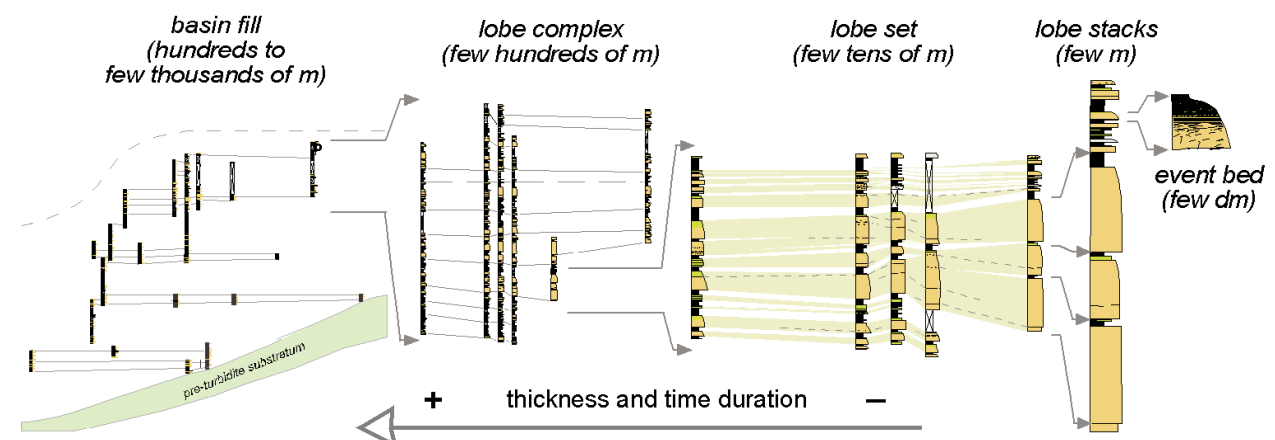


Fig. 11 - The Southern Laga Basin lobe succession broken down into components hierarchical orders. See the text for discussion.

The Poggio Umbricchio Lobe Complex (PUC)

This complex constitutes the upper part of the lower Laga 1 and crops out along the Vomano Valley between Aprati and Poggio Umbricchio. PUC pitches out to the E and S onlapping onto the western limb of the Montagnone Anticline and the Gran Sasso palaeoslope, respectively (see Figs. 12 and 16). Correlation of the measured sections with deposits W of the Mt. Gorzano normal fault has been carried out comparing the overall vertical trend in sand content vs. the gamma-ray log from the Campotosto exploration well (alias 44 in Figs. 4 and 5). The estimated maximum thickness of the Laga Fm from burial data (Bigi et al., 2009), together with sedimentary facies from this study, suggests that W of the Mt. Gorzano Normal Fault, deposition might have taken place in a tectonically-controlled, shallower minibasin as a result of synsedimentary activity of T2 and T3.

On the whole, 7 sections have been logged from PUC, 5 of which are aligned along a 9 km-long transect roughly perpendicular to mean palaeoflow direction. The remainder sections (91 and 92) have been logged on the eastern flank of the Mt. Gorzano to get insights on the more proximal sector of this complex.

Mean palaeoflow direction from sole casts is toward SSE (Fig. 12) with few palaeocurrents directed toward SE and E related to flows fed from the Campotosto sector. Palaeoflow direction from sedimentary structures varies in broader range. Few entries from current ripples are orthogonal or reverse with respect to the mean paleoflow direction from sole casts indicating a range of reflection or deflection off the slopes bounding the basin.

Geometric relationship of PUC lobes with basin margins (Fig. 12), size of the depocentre inferable from basin correlations and structural setting (Fig. 5) and occurrence of facies referable to channel lobe-transition settings (Facies L1), together suggest a very confined depocentre hosting turbidite systems with quite contracted physiography.

The Crognaleto Complex (CC)

As seen already for PUC, this complex (Fig. 13) onlaps the western limb of the Montagnone Anticline visibly pinching and shallowing out. Although the onlap of CC onto the Gran Sasso palaeoslope is not preserved because of tectonic deformation, linked to T2 and erosion, turbidity currents might have impinged roughly orthogonally onto it few Km to the S from the measured sections.

Comprehensively, five sections were logged and three revisited from the literature (Casnedi et al., 2006) in this lobe complex. In strike-section, correlations have been walked out in the field over approximately 8 km (right-hand side of panel in Fig. 13) along a quite continuous belt between Cesacastina and Case Vernesi, whilst in dip-section, they cover a 7 km-transect (left-hand side of panel in Fig. 13) through the axial sector of lobes.

Although CC continuity is interrupted by the Mt. Gorzano inverse fault, facies, thickness and sand content variation in strike-section (see data in Casnedi et al., 2006), suggest that, beyond its onlap onto the Montagnone Anticline, this lobe complex might have been topographically confined to the W either, as a result of tectonic uplift on the inner slope.

Palaeoflow direction from sole marks varies in a narrower range if compared to those of younger lobe complexes (see next paragraphs) and suggest deflection along the eastern basin margin. Paleocurrents from bedforms range from E to WSW, with few entries from ripples possibly testifying

reflection off the bounding slopes whilst small dunes form the most proximal section available (see section 70 in Figs. 13 and 17a) would indicate that turbidity currents were fed from the W.

Valle Vaccaro Lobe Complex (VVC)

In the study sector, this complex is represented by a mud-rich interval constituting the uppermost Laga 1 Unit. It shows a straightforward fining-thinning upward trend culminating in a thin, key-bed of carbonate micrite, which can be traced throughout the lobe sector and has been interpreted as the testimonial for the maximum sediment starvation affecting the turbidite basin (Milli et al., 2007).

Five sections have been measured along a 7.5-km transect nearly perpendicular to the mean paleoflow direction from sole casts (Fig. 14), which ranges from SSE to SSW. Palaeocurrents from ripples varies from ENE to S.

Along the Vomano Valley (Fig. 14) lobes of VVC spill toward the E over the Montagnone Anticline culmination (Fig. 16) suggesting that a considerable change in basin morphology and degree of topographic confinement might have taken place during the deposition of this complex. This is also recorded by palaeocurrents, which up-section rotate toward E as topography is smoothed out by turbidite sedimentation.

Facies, mud content and inferred basin morphology altogether allow interpreting this interval as the distal-lobe-fringe sector of an unconfined lobe complex.

The Mt. Bilanciere Lobe Complex (BC)

This complex covers an approximately 350 m-thick interval of the lowermost Laga 2 Unit and represent a complete cycle of lobe growth showing a coarsening-thickening upward trend in its lower part turning into a fining-thinning upward trend in its upper part.

Five sections have been logged from the lower part of this complex between Altovia (southern flank of Mt. Bilanciere) and Rocca S. Maria and correlated over an 8 km-long transect nearly perpendicular to the mean paleoflow direction (Fig. 15). Only two sections were logged from the upper part of this complex and correlated to those published by Mutti et al., 1978).

Palaeoflow direction from both sole casts and ripples ranges from SE to S with a mean value of N145°.

On ortho-aerial imagery, BC continuity can be traced laterally toward the NE up to its onlap onto the western limb of the Montagna dei Fiori Anticline (Fig. 16), which is located 4 km away from the easternmost section of Fig. 15. Geometrical relationship of the older VVC and mean palaeoflow direction from sole casts of BC (mean value N135°) altogether suggest that turbidity currents were no longer confined by the Montagnone Anticline and did not impinged orthogonally onto the Gran Sasso Paleoslope.

Facies spatial distribution

An example of facies spatial distribution in dip-section is shown by details in Fig. 16. These details cut lobes of the Crognaleto Complex in an axial (Fig. 17a) and a more peripheral (Fig. 17b) position and cross the panels of Fig. 18 in correspondence of section 71 and 74, respectively. Is worth to note how in Fig. 17a all of the thickest sandstone beds reach their maximum thickness in section 60 giving rise to lenticular shapes. This downstream thickening is

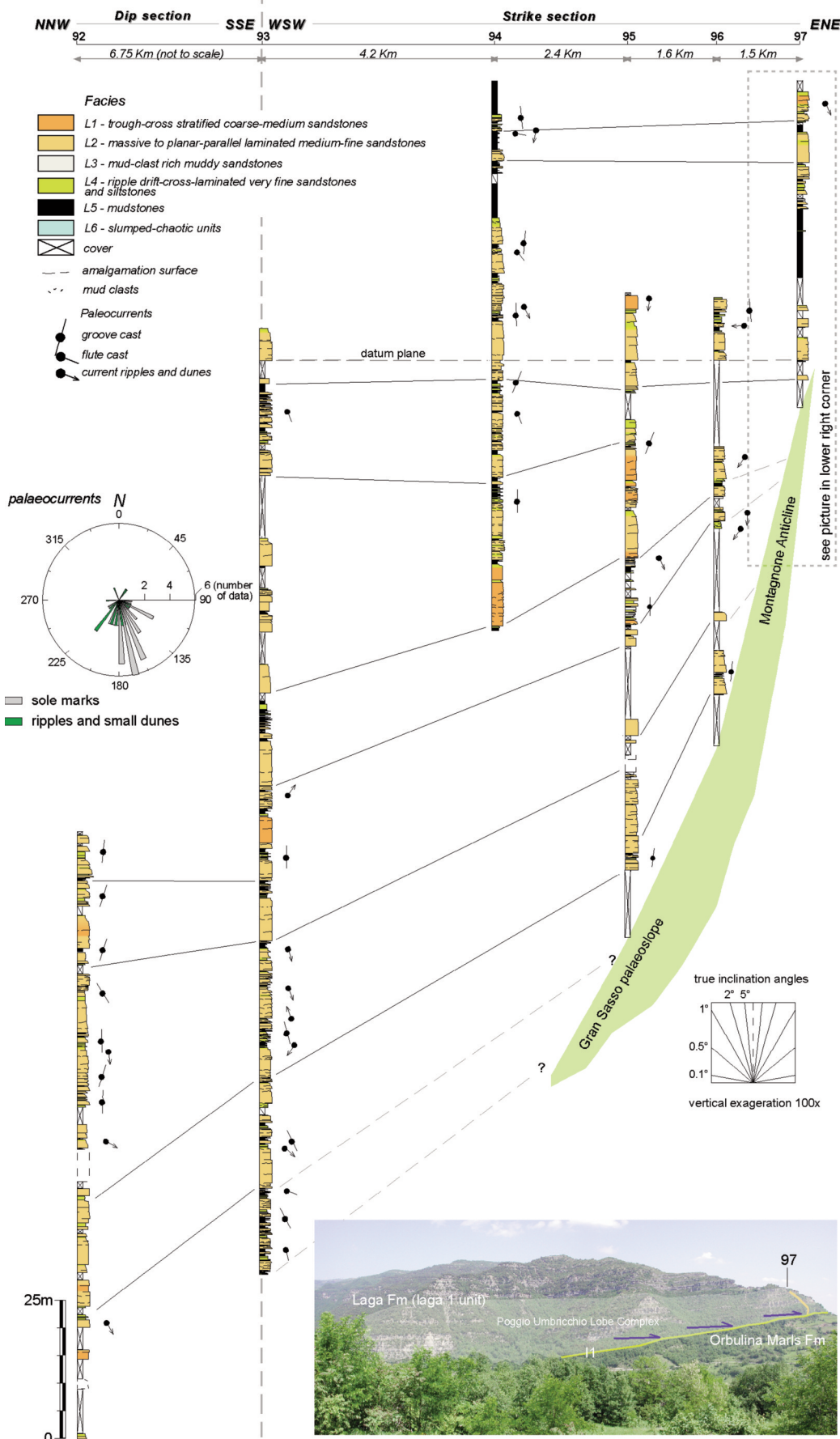


Fig. 12 - Correlation panel through the Poggio Umbricchio lobe Complex. Mean paleocurrent direction is toward the right and toward the viewer on the left-hand and right-hand sides, respectively. The picture in the lower right corner shows the Laga 1 lobes onlapping onto the pre-turbidite substratum. Note the tabularity of beds and sheet-like architecture of the succession.

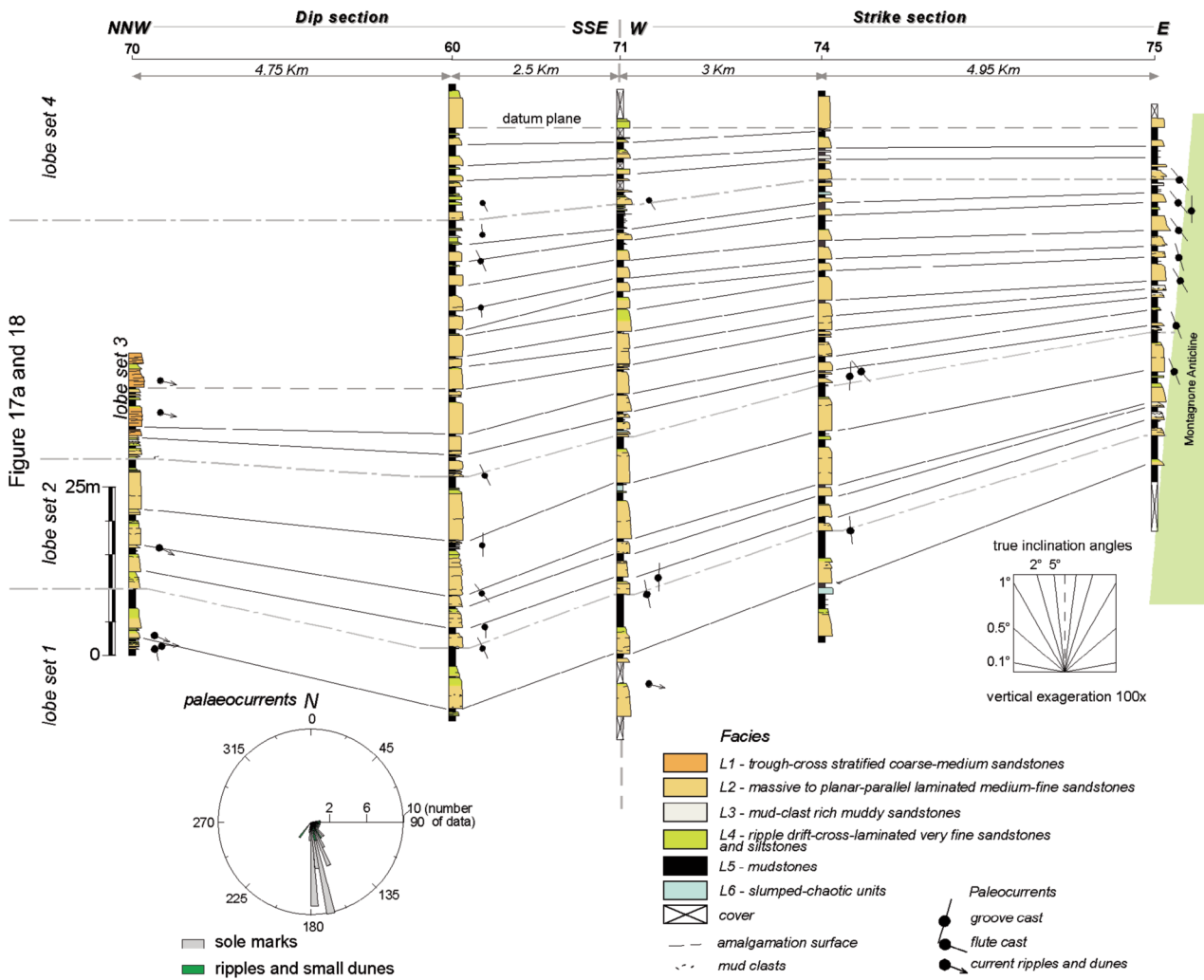


Fig. 13 - Correlation panel through the Crognaleto lobe Complex. Mean paleocurrent direction is toward the right and toward the viewer on the left-hand and right-hand sides, respectively. Note the tabularity of beds and the sheet-like architecture of the complex.

accompanied in lobe-set 3 by transition from trough-cross stratified sandstones of facies L1 to massive-laminated sandstone of facies L2 and would indicate a consistent sediment bypassing in proximal lobe settings.

Downstream of section 60 (Fig. 17a) and section 69 (Fig. 17b) sandstone beds thin and shale out (see facies cumulative thickness).

In section 60 (lobe-set 2) and 71 (lobe-set 3) occurrence of facies L3 downstream of facies L2 on top of very thick, lenticular sandstone bodies, is consistent with flow blocking by depositional microtopography (see interpretation of facies L3).

Depositional microtopography is also responsible for sediment instability of sediments at the lobe front as testified by slumped beds of facies L6 occurring in section 71 (Fig. 17a, lobe set 3) at the top of a very thick, lenticular lobe stack.

Although in details of Fig. 17b changes of sandstone bodies characteristics are less marked than that observed in detail a, all of the sandstone beds show a subtle thinning out downstream of section 69 and cumulative sand content decreases (see pie charts) mainly for shaling out of facies L2 and L4. Moreover, owing to the position of the available sections with respect to the eastern basin margin (Fig. 16), facies L3 and L6 are relatively suggesting a leading the role of basin topography in favouring flow transformations and

seafloor gravitational instability.

As a whole, stacking patterns of beds and facies sequences in along-dip clearly show the stages of lobe growth consisting of an early progradational phase, followed by a late phase of retrogradational and facies back-stepping.

Details of Figs. 18 and 20 allow exploring facies transitions in strike-section and compare the architecture of the Crognaleto and the Mt. Bilanciere lobe Complex as end-members of topographic confinement.

Because of a prominent confining topography and a smaller depocentre size, the lobe sets of the Crognaleto Complex have a strongly layered architecture (see Fig. 13) and rapidly pinch and shale-out toward the E. In lobe sets 2 and 3 (Fig. 18) facies cumulative thicknesses show a remarkable increase toward the E in the L3/L2 and L5/L2 ratios, which suggests deceleration of at least the more concentrated, basal part of turbidity currents forced by bounding slopes.

Cumulative thickness of L4 changes toward the E only slightly in favour of L5, consistently with the ability of low-concentration clouds to running up the confining slopes.

As concerns L6 beds, they occur exclusively in mud-prone intervals (i.e. in lobe-fringe facies associations) at the top of thick lobe stacks and are rarely found in the most easterly section of Fig. 18. Combining strike and dip sections (see also

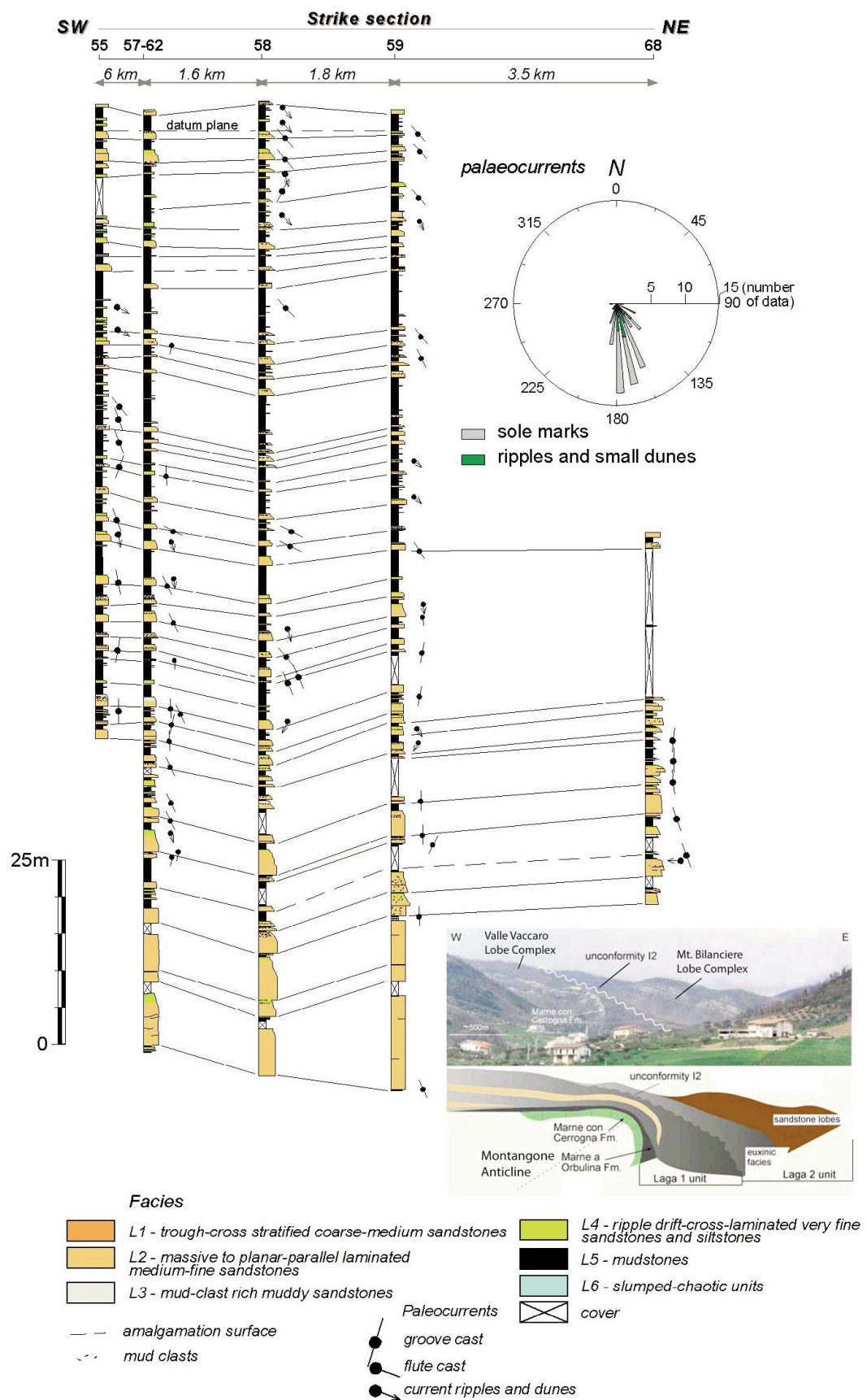


Fig. 14 - Correlation panel through the Valle Vaccaro lobe Complex. Mean paleocurrent direction is toward the viewer. The picture in the lower right corner (modified after Artoni, 2003) shows the geometrical relationship between the lobes of the Valle Vaccaro and Mt. Bilanciere complexes and the Montagnone Anticline.

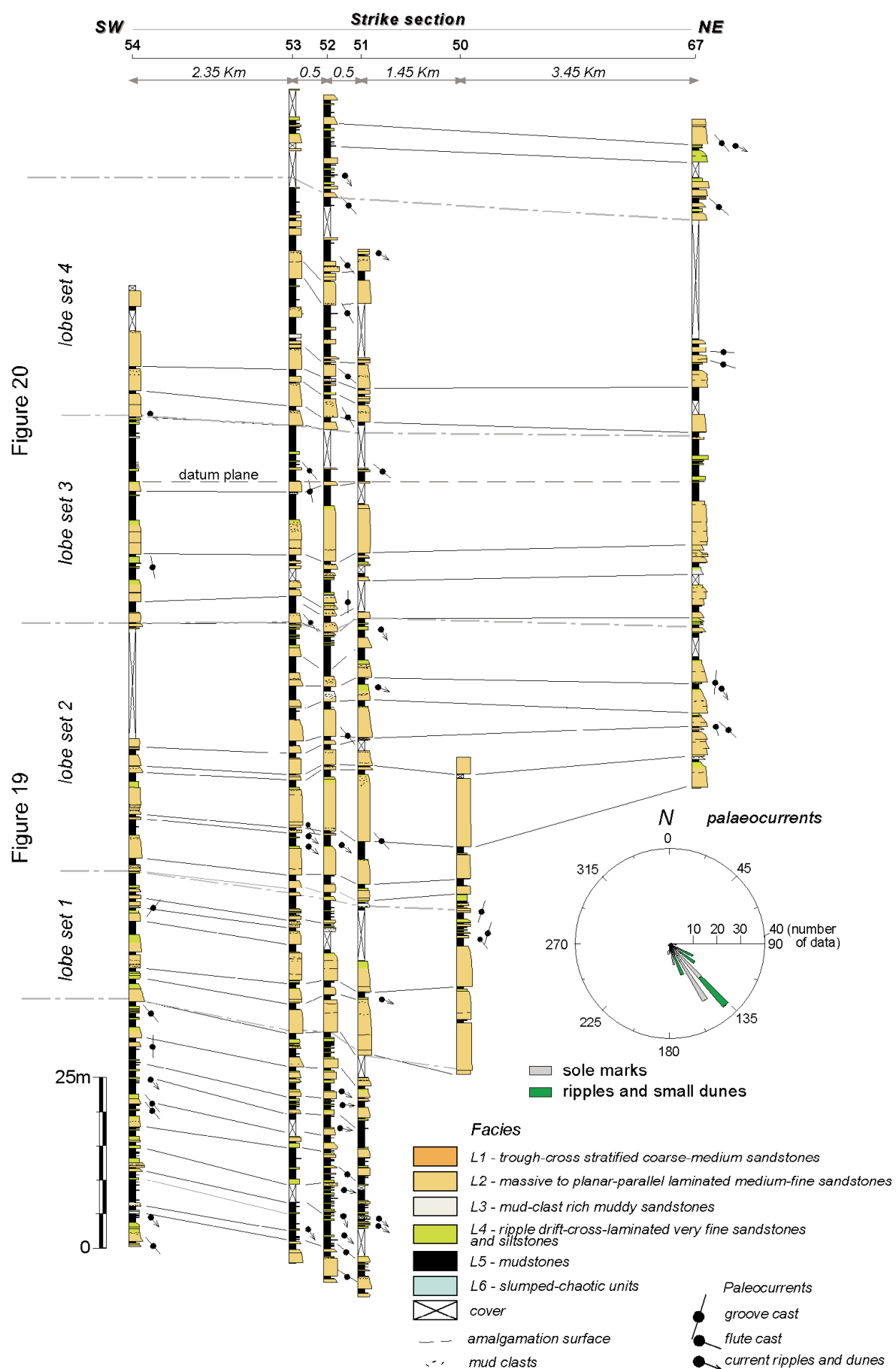


Fig. 15 - Correlation panel through the Mt. Bilanciere lobe Complex. Mean paleocurrent direction is toward the viewer.

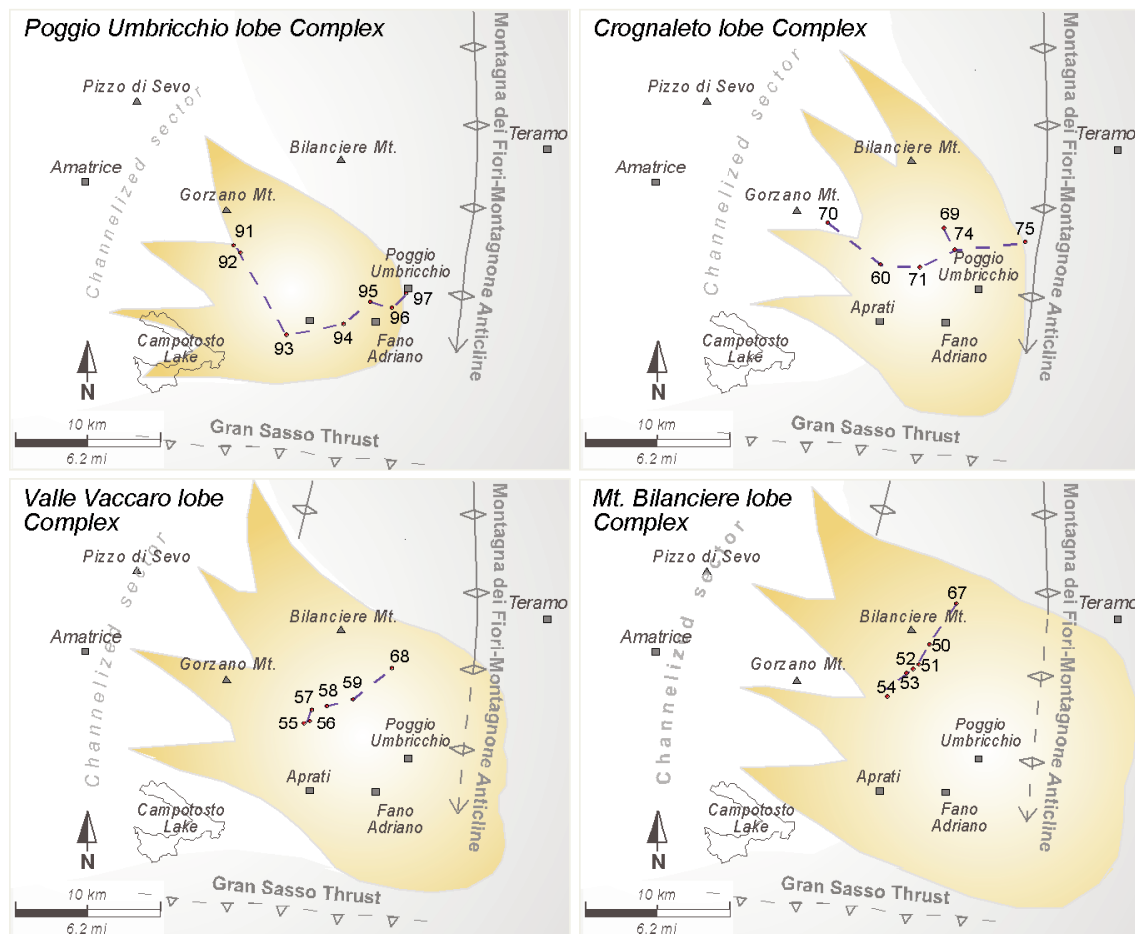


Fig. 16 - Simplified sketch showing the inferred areal extension of the studied lobes complexes and the location of measured sections and correlation panels of Figs. from 12 to 20.

Fig. 17), it can be hypothesized that the topography causing gravitational instability of slumped TBT packages might have been quite articulated, being the result of the combination of basin morphology and three-dimensional geometry of lobe stacks.

Although the Mt. Bilanciere Complex shows a subtle pinch-out at basin margin toward the NE (see Fig. 15), the sand/mud ratio is almost constant in strike-section mainly because of the spatial stacking of lower-hierarchy component units. Indeed, as can be observed in Figs. 19 and Fig. 20, as upbuilding of lenticular lobe stacks and lobe sets makes for uneven seafloor microtopography, successive units partially compensate such topography pinching out toward highs. Beyond pinch-outs, the effect of flow interaction with depositional microtopography is testified by spatial distribution of L3, which occurs either at flanks or on tops of depositional highs.

Moving toward lobe stacks peripheries, lateral transition of massive - laminated sandstones (L2) to ripple-drift cross laminated sandstones (L4) and mudstones (L5) is more marked than that seen in the confined Cognaleto Complex and might have resulted from free lateral spreading of flows in an unconfined depositional setting.

Similarly to what observed in the Cognaleto Complex, L6 beds from the Bilanciere Mt. Complex occur in mud-prone intervals but on flanks of lenticular lobe stacks; this would suggest a probable strong control on sediment remobilisation by depositional topography.

Sandbody geometries

Mostly because of outcropping conditions, available data allow us describing systematically only strike-section shapes of sandstone bodies. Nonetheless, the few along-dip correlations available still enable to draw some considerations on three-dimensional geometries and mode of lobe growth. Data from the Poggio Umbricchio Complex were discarded owing to the poor expositions of this interval, which does not allow a reliable correlation framework.

Although all of the sandstone bodies appear nearly tabular in both strike and dip section at the outcrop-scale, their profile varies within a quite broad range instead. This is much clearer as we either introduce vertical exaggeration in correlation panels (Figs. 17 and 20) or plot sandbody thickness measured on sections against distance (Fig. 21).

It should be noted that the sample comprises both event beds and composite sandstone bodies (i.e. lobe stacks), which can be tentatively discriminated on the graphs of Fig. 21 by a reference line marking the maximum thickness observed for event beds in the studied interval. This also allows evidencing the dependency of sandbody geometry on thickness, and hence, on their hierarchical order.

Very thick, lens-shaped lobe stacks with prominent upward convexity occur at different levels in the Mt. Bilanciere Complex and at the base of the Valle Vaccaro Complex (see Figs. 14 and 15). As can be inferred from correlations (Figs. 19 and 20), the arrangement of amalgamation surfaces within

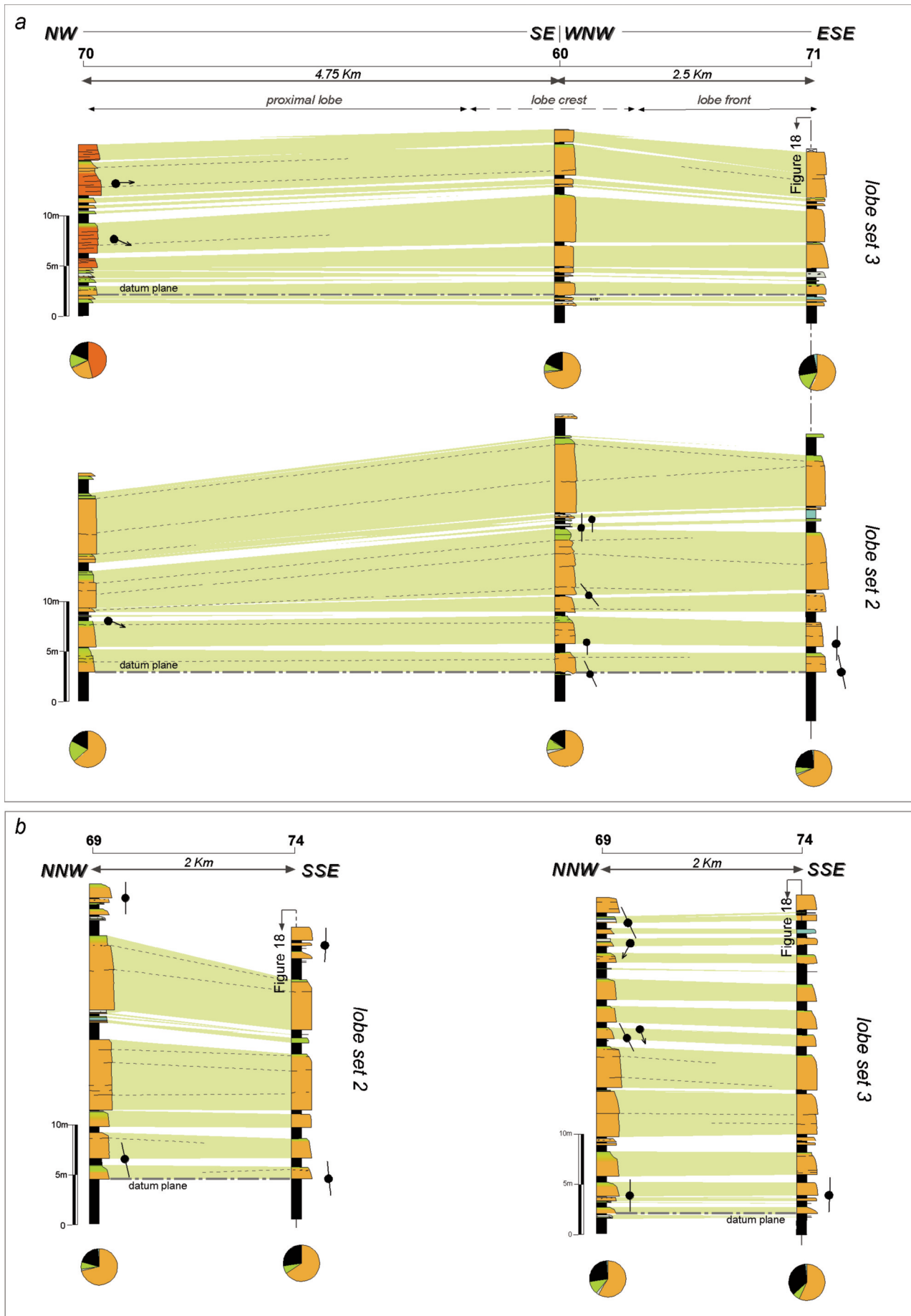


Fig. 17 - Dip-sections through the lobe sets 2 and 3 from the Crognaleto Complex.

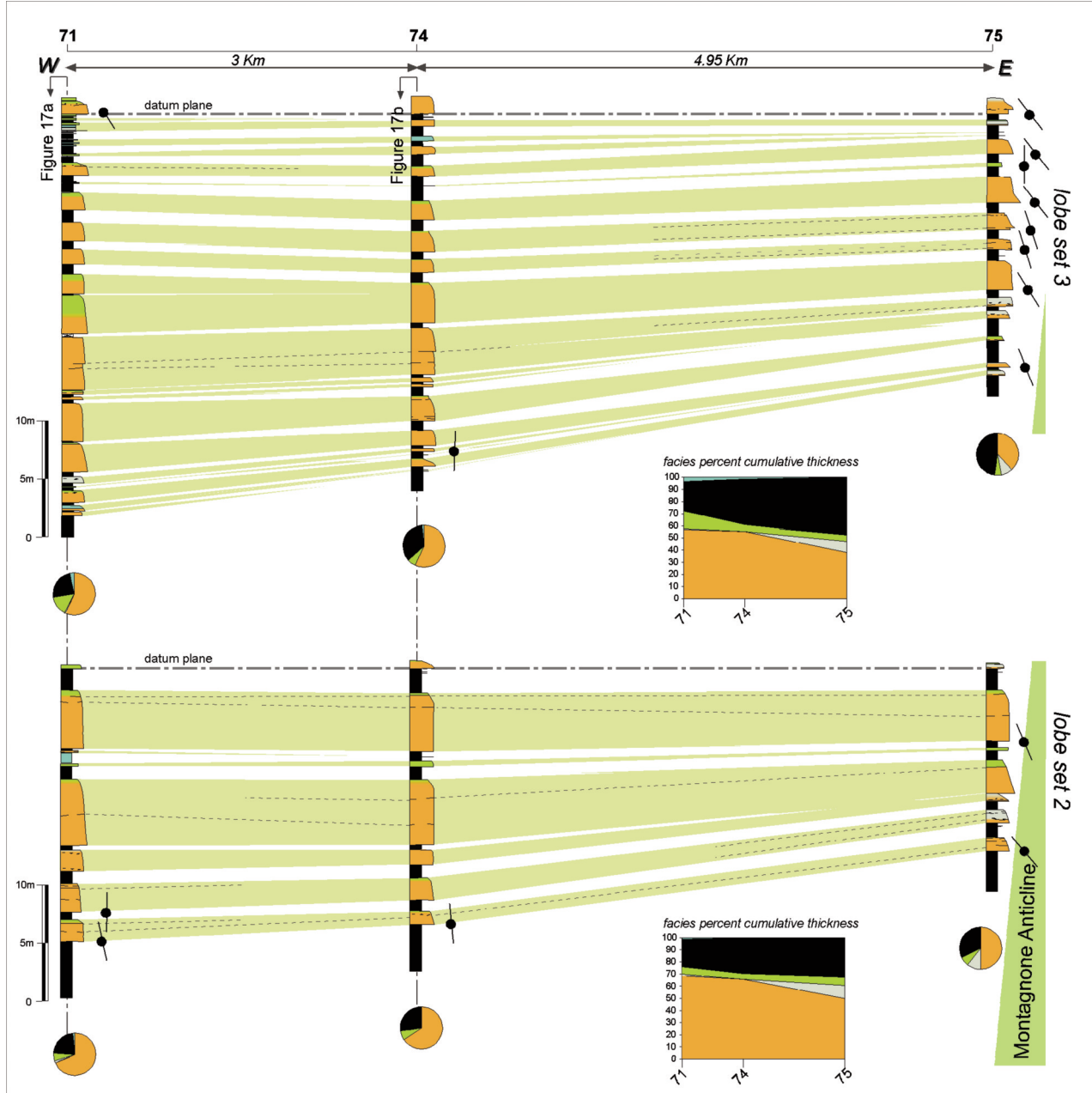


Fig. 18 - Strike-sections through the lobe sets 2 and 3 from the Crognaleto Complex.

these sandstone bodies strongly suggests a shingled-stacking of component event beds. This internal organisation of lobe stacks can be regarded as the result of partial compensation of seafloor topography by successive depositional events, a process in turn giving rise to vertical aggradational and lateral accretion of lobe stacks themselves (Fig. 22).

Thinner lobe stacks and event beds with convex downward shape or irregular "pinch and swell" shapes mostly occur at the flanks or top of the aforementioned lens-shaped lobe stacks and taper out against their flanks. The overall shape of these sandstone bodies clearly indicate compensation of seafloor topography and are found almost exclusively in the Mt. Bilanciere Complex (Figs. 19 and 20).

The remainder sandstones bodies from the Mt. Bilanciere Complex and the totality of those from the Crognaleto and The Valle Vaccaro complexes show a nearly tabular strike-section shapes and range in thickness and hierarchy from very

thin event beds to very thick lobe stacks. Especially in lobe stacks from the Crognaleto Complex (Fig. 18), the arrangement of internal amalgamation surfaces indicates simple vertical stacking of indicates simple event beds, which might have essentially produced the aggradational of lobes (Fig. 22).

Despite their tabularity at the scale of few km, almost all of the beds from the Crognaleto Complex taper out at higher rates between sections 74 and 75, i.e. in the close reach of the eastern basin margin (Figs. 18 and 21b). This may be interpreted as a short-reach effect of turbidity currents interaction with the confining lateral slope.

Given the different depositional setting of the studied complexes, the graph of Fig. 21 also consents to interpret the differences in bed geometry in terms of proximality and degree of topographic confinement. For instance, it can be easily noted how sandstone bodies from the confined

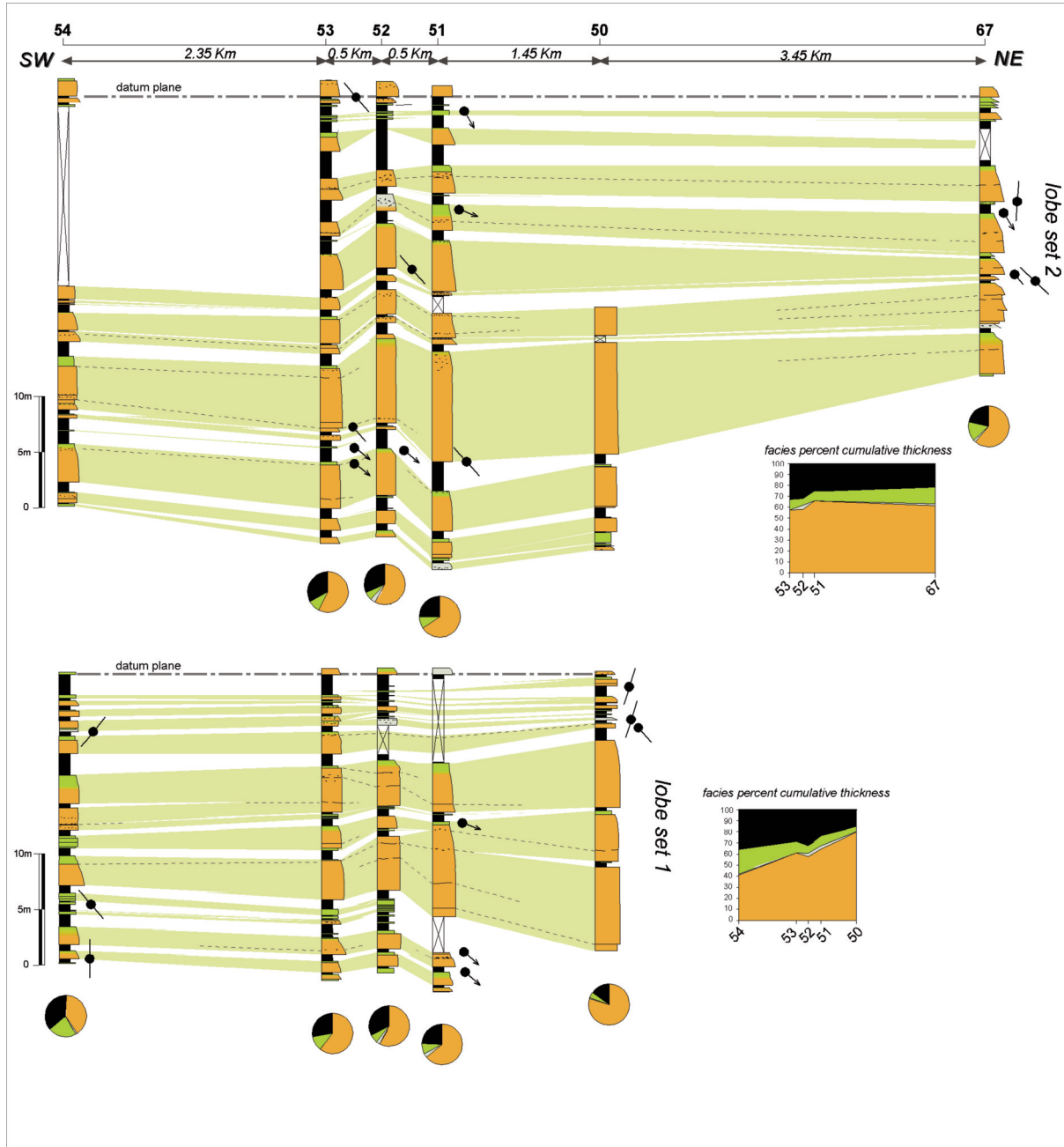


Fig. 19 - Strike-sections through the lobe sets 1 and 2 from the Bilanciere Mt. Complex.

Crognaleto Complex are more tabular than those from the unconfined Mt. Bilanciere Complex and show quite regular strike-section shapes. Toward their peripheries, these pitch out as a result of turbidity current interaction with the lateral bounding slope. Also, the beds from the Valle Vaccaro Complex, which has been referred to a distal lobe setting, are rarely thicker than 2 m and notably more tabular than those lobe stacks from the other complexes.

Dip-sections of Fig. 17 depict two lobe sub-stages (sensu Mutti and Normark, 1987, 1991) from the Crognaleto Complex and allow visualizing the main features of the along-paleoflow profile of component sandbodies. The down-current thickening of event beds and lobe stacks in the proximal half of these details (left-hand side of Fig. 17), which in lobe set 3 is accompanied by transition of trough-cross stratified coarse-grained sandstones (L2) to fine-grained massive-to-laminated sandstone of L2, suggests a

channel-lobe transition or, at least, a proximal lobe setting of deposition. Downstream from section 60, where the majority of beds reach their maximum thickness, especially lobe stacks thin and significantly shale out further downstream consistently with transition from proximal to distal lobe settings. In this sector, which can be referred to as lobe front, the sum of depositional topography and seafloor slope may determine the condition for gravitational instability of heterolithic intervals (see section 60 in lobe set 3 of Fig. 17).

However, some of the dip-section shapes form the Upper Mt. Bilanciere Complex as far more complicated than those from the Crognaleto Complex because of geometrical compensation of complex, 3D geometries. This highlights the need of more control point to constrain geometries and event beds stacking rules when 3D planform and compensational processes are documented by bed-by-bed correlations.

Concerning the mode of depositional lobe growth, lobe

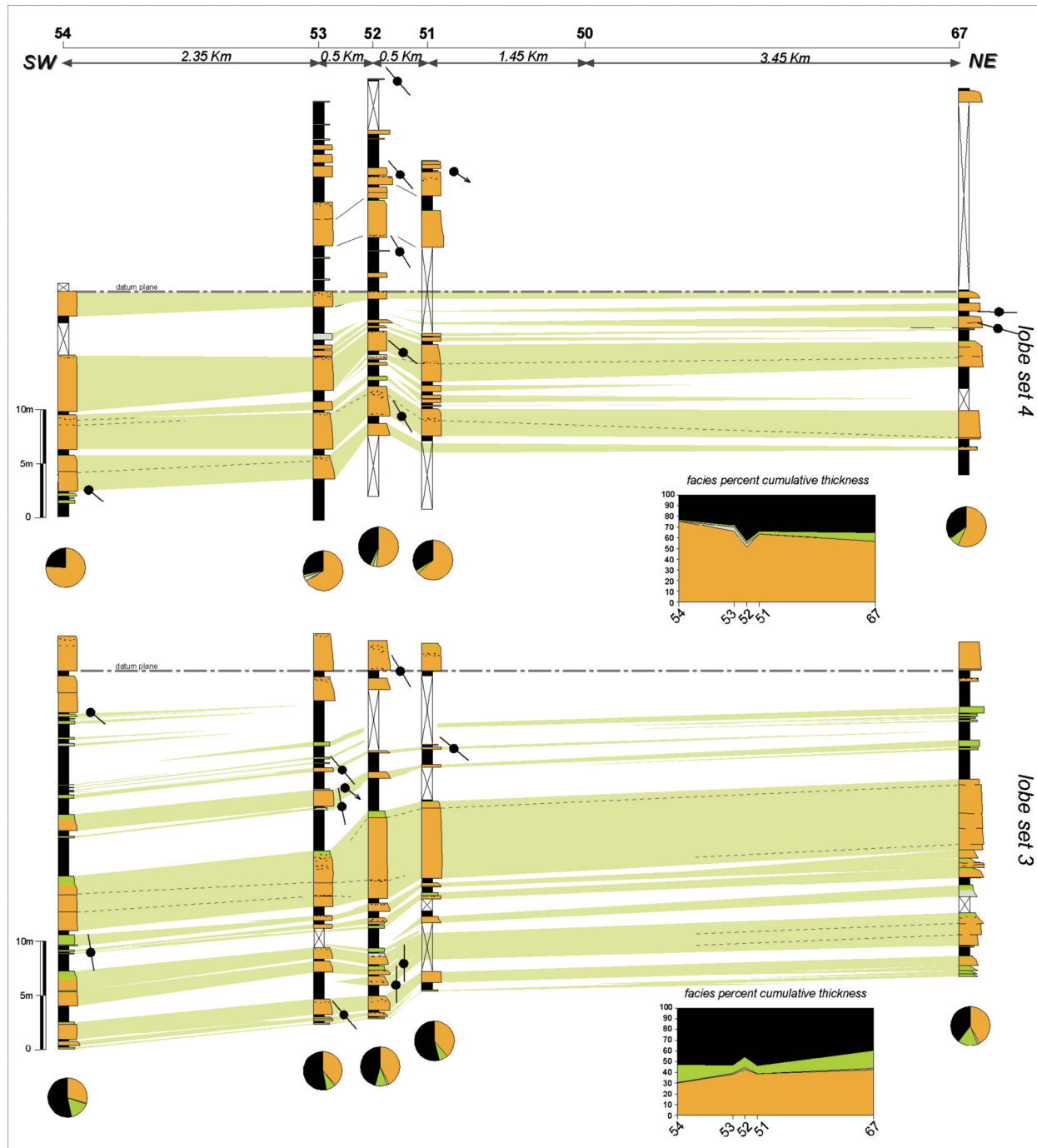


Fig. 20 - Strike-sections through the lobe sets 3 and 4 from the Bilanciere Mt. Complex.

sets of Fig. 17 show a clear progradational character reflected by thickening-coarsening upward trends in their lower part, followed by a steeper opposite trend in their upper part. At the smaller scale, individual lobe stacks show a similar internal organisation, which is often undetectable for complete welding of event beds, constancy of grain-size or for diagenetic obliteration. However, on particularly well exposed outcrops, the spacing of amalgamation surfaces in the basal, coarser-grained part of lobe stacks increases upward until amalgamation surfaces disappear or cannot be detected any longer. Moving further upward, amalgamation surfaces show up again and bound thinner and finer-grained beds. Finally, the upper part of lobe stacks is represented by heterolithic intervals which record the sudden retrogradation

of the system.

The prograding nature of both lobe sets and lobe stacks can be explained by variation in sediment delivery to depositional lobes possibly related to climate or autocyclic processes such as channel avulsion in proximal sectors of turbidite systems or local compensational processes.

DICUSSION

Facies and processes

Facies spatial relationship and inferred depositional processes presented in previous paragraphs are summarized in Fig. 23.

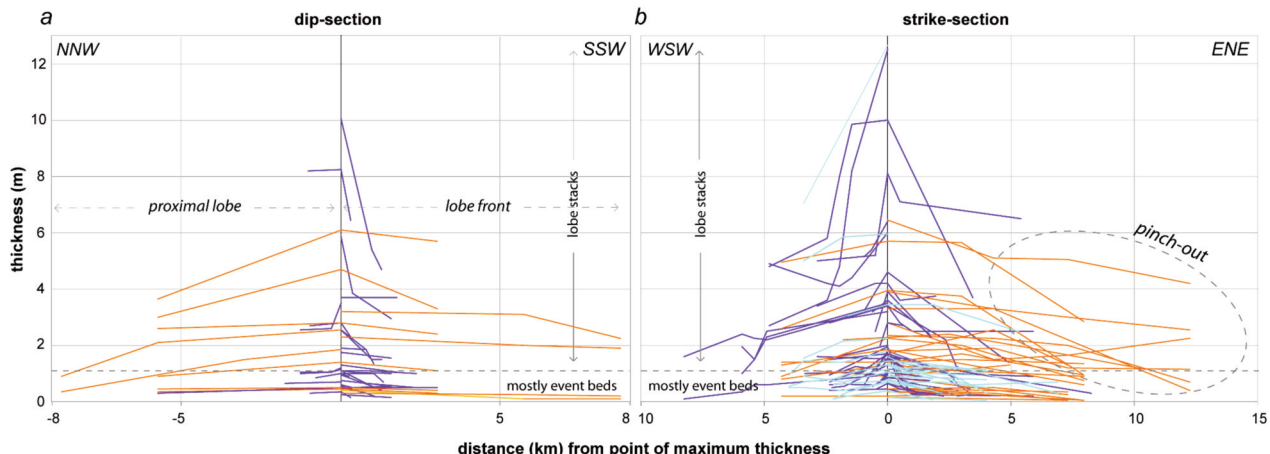


Fig. 21 - Dip (a) and strike (b) profiles of sandstone body thickness from the Crognaleto Complex (orange lines), the Valle Vaccaro Complex (turquoise lines) and the Mt. Bilanciere Complex. Sandstone body thickness is plotted against distance from the section where maximum thickness was measured. Colored connect lines, which linearly interpolate data points, show the gross shape of event beds (below the dashed line) and lobe stacks (above the dashed line). Note the pinching out of lobe stacks from the Crognaleto Complex toward the eastern basin margin.

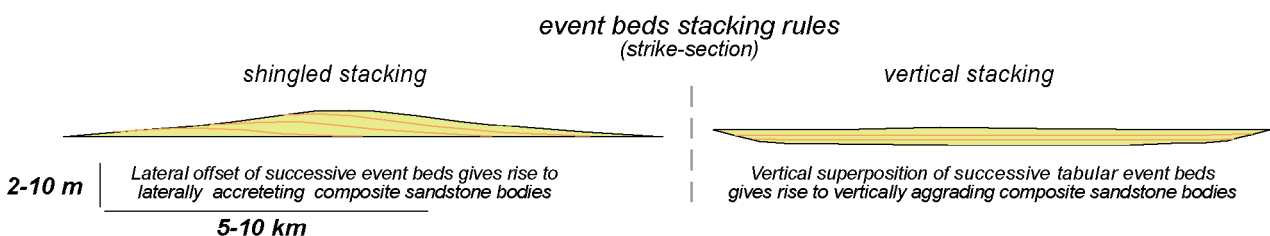


Fig. 22 - Cartoon showing two different modes of strike-section spatial stacking for successive event beds.

Genetic interpretation of L1 is based on its relationship with both classical, Bouma sequence (facies L2, L4 and L5) and channalized deposits cropping out in the Northern Laga Basin (Milli et al., 2007; Bigi et al., 2009). Differently from what suggested by some Authors for similar facies (e.g. Mutti et al., 1999) occurring in alike depositional settings (Facies E in Mutti and Ricchi Lucchi, 1972; Mutti, 1977 and Mutti and Normark, 1987; Facies B2.2 in Pickering et al., 1986; Facies F6 in Mutti, 1992 and Mutti et al., 1999), we suggest that thick L1 beds should not be interpreted as the product of long-lived (i.e. sustained flows sensu Kneller and Branney, 1995), large-volume turbidity currents, but rather of several discrete depositional/reworking events by bypassing turbidity currents in a channel-lobe transition sector or in proximal lobes. Indeed, L1 beds described in this study are made up of bundles of trough-cross stratified sandstones that can be traced distally into individual event beds of massive to laminated sandstones and require persistency of adequate hydrodynamic conditions for a certain number of successive turbidity currents to be explained. In a sand-rich turbidite system like those from the Laga Basin, such conditions are likely to be met in correspondence of a gradient break in the along-dip profile of the system where flows switch from erosive to net depositional behaviour and abandon the coarsest part of their load bypassing to terminal splays (i.e. depositional lobes). In this case study, bypass associated to L1 does not produce a significant physical detachment of finer grained facies. On the contrary, basin-scale correlations highlight a clear physical continuity between channelized deposits and depositional lobes, which is a feature commonly observed in sand-rich systems of oversupplied,

confined basins.

The genetic interpretation of L2 coincides with that widely accepted in the literature invoking a range of conditions from quick, en-masse deposition to traction on a plane bed in supercritical conditions (see Mutti, 1992 for a review). Nonetheless, in our view deposition of L2 is not related to high-density flows (Lowe, 1982) but rather to the high concentrated basal layer of turbidity currents s.s. In agreement with the widespread occurrence of L2 sandstones down-current of L1 in proximal and channel-lobe transition sectors, massive-to-crudely laminated intervals of L2 are here explained as the result of quick deposition for sudden loss of momentum by turbid currents at channel mouths, i.e. where they switch from confined to unconfined flow condition (see also Falcini et al., 2009). Moreover, abundance of massive L2 in the lower part of the studied succession (Poggio Umbicchio and Crognaleto Complexes) suggests that flow blocking at basin margins may have locally induced a sufficiently high settling rate to suppress traction at the water-sediment interface.

In this study, L4 is interpreted as the product of traction-fall out processes by low concentration turbidity currents and trailing tail of other flow types. Few palaeoflow data from the Poggio Umbicchio and Crognaleto complexes indicate flow deflection and reflection off basin margins, a process already acknowledged by the literature (Kneller et al., 1991; Kneller and McCaffrey, 1999; Sinclair, 1994; Remacha et al., 2005) from a number of confined basin and demonstrated experimentally (Pantin and Leeder, 1987; Kneller et al., 1997).

Finally, downstream of L4, deposition of L5 mudstones registers the end deceleration of the most dilute part of

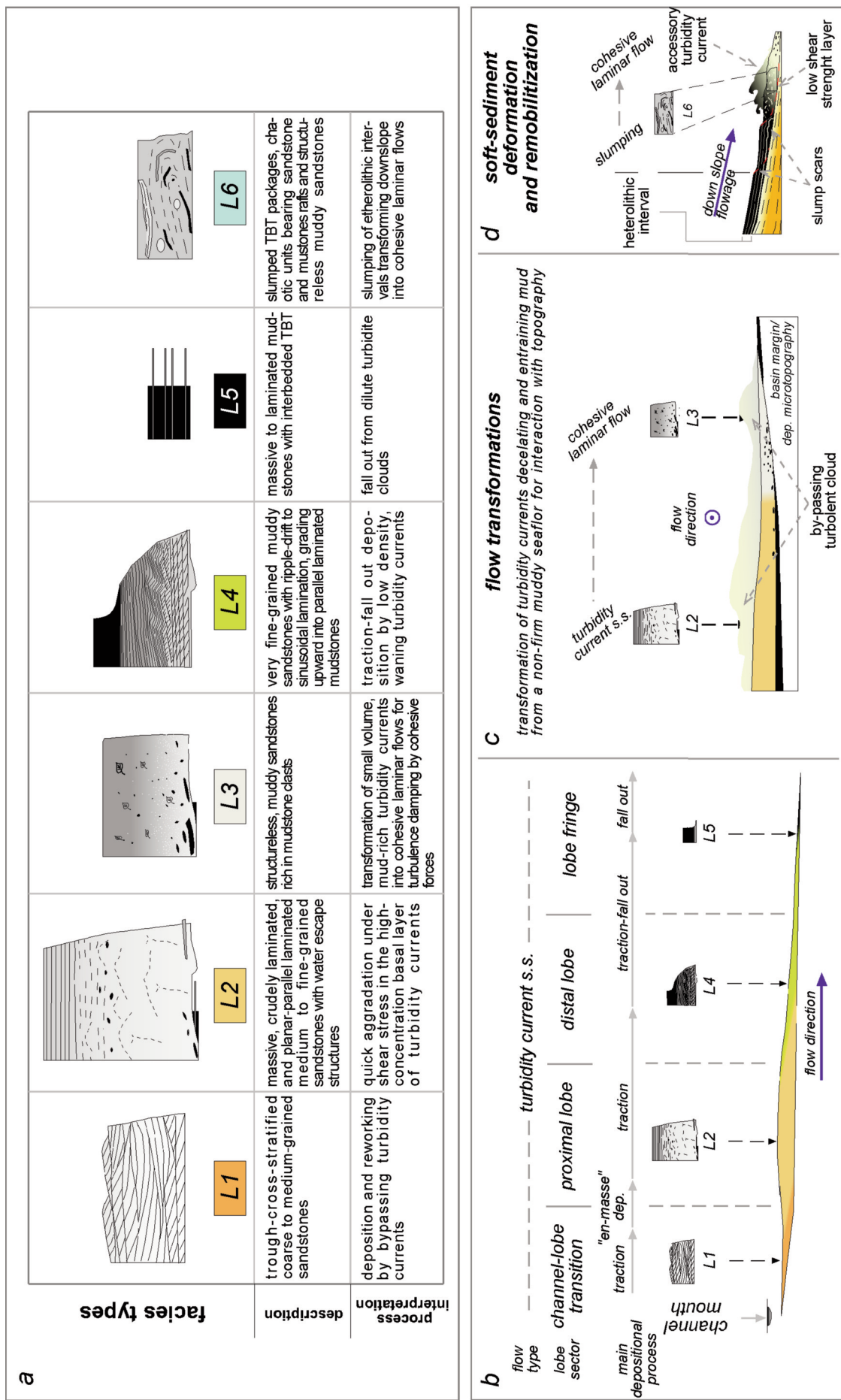


Fig. 23 - Facies types (a) and facies tracts (b-c) for the deposits making up the lower Messinian lobe complexes from the Southern Laga Basin.

turbidity currents, which were possibly affected by ponding by basin topography especially for relatively large, mud-rich flows.

Despite their limited volumetric relevance, facies L3 and L6 can be accounted as very good proxies for inferring a certain seafloor topography.

The depositional processes invoked in this paper to explain the occurrence of facies L3 were early hypothesized by other workers in reference to slurried beds from the Marnoso-arenacea Fm. (Ricchi Lucchi, 1978; Ricci Lucchi and Valmori, 1980). Slurried beds of these Authors had a peculiar tripartite structure, consisting of an ungraded muddy sandstone interval (or slurried interval, that is, the facies L3 of this study) sandwitched by clean, laminated sandstones. Relevantly to the specific study area of the present work, Mutti et al. (1978) described few slurried beds from the Mt. Bilanciere turbidite succession occurring on flanks of sandy depositional bulges (e.g. lenticular, thick lobe stacks). These were interpreted as the product of large turbidity currents eroding mud from the top of depositional bulges the redepositing sand-clay slurries under highly viscous flow condition within local or subsidiary debris flows incorporated in their tails.

If these early attempts to explain the origin of slurried beds already placed a strong emphasis on their peculiar tripartite structure, more recently (Haughton et al., 2003, 2009; Talling et al., 2004; Davis et al., 2009) this was explained with co-genetic models. In such models, integrating some of the concepts already put forward by Lowe and Guy (2000) and Lowe et al. (2003), deposition of the basal turbidite bed and the overlying, mud clasts-rich, muddy sandstones would record the transformation from a fully turbulent flow to a laminar cohesive flow occurring in response to mud entrainment and turbulence suppression by cohesive forces. Finally, the thin bed at the top of the slurried unit would constitute the product of the dilute turbulent tail of the flow.

In this study, the occurrence of L3 beds in proximity of the eastern basin margin (see Fig. 18) and on flanks of depositional bulges (see Figs. 19 and 20) suggests a leading role of seafloor topography on deposition of this facies. Our genetic interpretation of L3 stems especially from these field evidences and attempts to council co-genetic models (Haughton et al., 2003, 2009; Talling et al., 2004) with those emphasizing the role of topography (Muzzi Magalhaes and Tinterri, 2010 and reference therein). In this interpretation, a relatively small-volume, decelerating turbidity current entrains cohesive sediments by eroding a non-firm muddy seafloor; erosion of either non-consolidated mud and mudstone clasts may be enhanced by flow interaction with seafloor microtopography or basin morphology, which, moreover, force the flow to dissipate momentum and decelerate over short distances. Deceleration and turbulent energy dissipation in turn may greatly reduce the efficiency of elutriation of fine-grained particles (among which clay minerals) determining an increase in cohesive particles concentration at least in the basal and more concentrated part of the flow. As demonstrated by experimental data (Amy et al., 2006; Baas et al., 2009), above a critical value of concentration, cohesive forces will prevail interlocking particles and suppressing turbulence to force a flow transformation from an initial fully turbulent flow to a laminar, cohesive flow, i.e. a debris flow sensu Postma (1986).

Although our field data show that often L3 beds cap L2 beds and are in turn capped by L4 ripple-drift laminated sandstones, this is not always the case: in some instances,

intervening mudstones separate the basal L2 division from the debrite-like L3 division indicating rather amalgamation of two distinct depositional events took place. This suggests that if the co-genetic models well explains theoretically the vertical association of slurried intervals and genuine turbidite facies, it should be applied carefully and from case to case. The tripartite structure of slurried beds may in fact represent *tout court* a facies sequence denoting, at a given observation point, the change in time of volume, physical structure and rheology of flows.

While slump and debris flow deposits such as those of L6 have been already described from a number of contexts, their occurrence in outer lobe or lobe fringe settings is striking unless we assume proximity to some topographic feature of the basin. The field examples from this study suggest that the presence of sediments yielding very low shear strength (such as those of L3) in heterolithic intervals, may favour slumping of the overlying non-consolidated sediments over very low-gradient slopes, such as those associated to depositional microtopography (e.g. at the lobe front, as in Fig. 17). The downstream transformation of these slumps into cohesive debris for dilution and progressive sediment mixing may originate both chaotic beds and muddy sandstones resembling those of L3.

Finally, the comparison of strike-sections through the lobe of confined and unconfined complexes clearly shows two distinctive patterns of facies and sand distribution. In confined lobes (such as the Crognaleto Complex) flow interaction with bounding slopes results in a straightforward decrease in sand content and an appreciable increase in muddy sandstone cumulative percentage toward marginal settings. On the contrary, in less confined or unconfined lobes (such as the Bilanciere Complex) facies distribution and overall sand content is less predictable and mainly depends on autocyclic processes, such as compensation of depositional topography, or allocyclic events affecting up-dip sectors of turbidite systems.

Depositional geometries and overall architecture of lobes from the Laga Basin

The observations made at different hierarchical scales from event beds to lobe complexes, allowed exploring the rules governing the spatial stacking of event beds and at a larger scale, the overall architecture of turbidite lobes from the Laga Basin.

If in strike section the geometry of event beds, which we assume to have lobate planform with upward convexity, changes mainly as function of proximity to channel mouths, that of lobe stacks is greatly controlled by the mode successive event beds are stacked spatially. This study suggests that the lobe stack build up may essentially reflect:

- i) Ineffective compensation of microtopography, which in strike-section results in a shingled-stacking of lenticular event beds and lateral accretion of highly lenticular lobe stacks;
- ii) Vertical stacking of low-lenticularity to nearly tabular event beds, which results in an overall aggradation of low-lenticularity lobe stacks.

Detailed bed - by - bed correlations show that shingled-stacking of event beds characterizes exclusively the proximal sector of depositional lobes and has mainly to do with flow with depositional microtopography. Indeed, depositional bulges forming in the early stage of lobe growth for sudden loss of competence by turbidity currents at channel mouths, may have blocked at least the more concentrated basal part

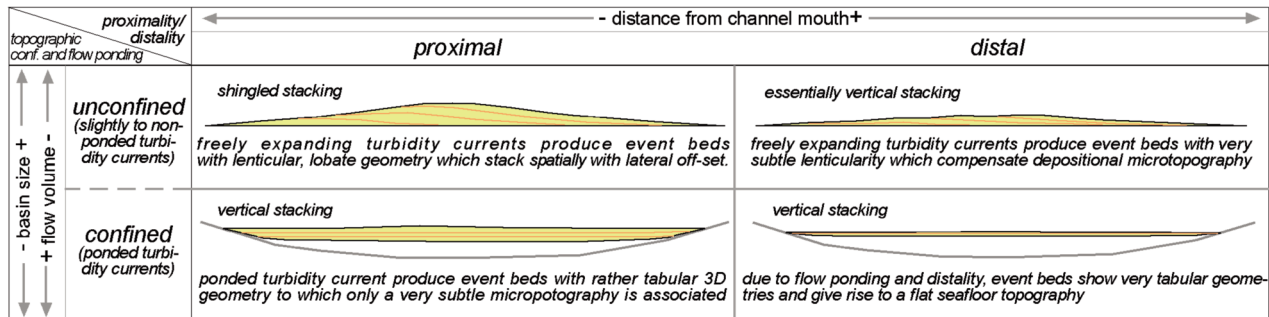


Fig. 24 - Mode of spatial stacking of successive event beds in strike section as function of proximity to channel mouth and basin confinement controlling in turn the degree to which turbidity currents are ponded.

of the successive events forcing them to abandon their load. Flow blocking around these bulges may have prevented compensation of seafloor microtopography and favoured lateral accretion of lobe stacks (Fig. 24) through shingled stacking of event beds.

Vertical stacking is the most obvious mode to stack spatially low-lenticularity to nearly tabular event beds, such as those typical of outer lobes or lobe fringes, and easily explain the up-built of low-lenticularity lobe stacks.

This explanation for lobe stacks geometry places a strong emphasis on proximality-distality and agrees with the three-dimensional geometry of unconfined lobes from modern fans (see data in Deptuck et al., 2008) and experimental results (Luthi, 1981; Alexander and Morris, 1994; Kneller, 1995).

Nonetheless, comparing the depositional geometry and internal organisation of lobe stacks from the examples of confined and unconfined lobes presented in this study, we propose an alternative model for explaining whether a composite sandbodies develop a marked lenticular geometry or a more flat one.

In our interpretation, we suggest that in confined lobes, flow ponding processes may favour deposition of event beds whose three-dimensional geometry is flatter than that of unobstructed turbidity currents from unconfined settings. Accordingly, stacking of successive event beds would give rise to rather flat lobe stacks in whichever sector of confined lobe. On the contrary, in unconfined lobes lenticularity of lobe stacks in proximal sectors would result from ineffective compensation of successive event beds (Fig. 25).

As shown by the few data available in dip-section, lobe-stacks and lobe sets essentially grow through a forestepping-backstepping stacking of event beds and lobe stacks (Fig. 25), respectively. This high-frequency cyclicity, which in our case study is straightforward throughout the studied interval, appears to be primarily controlled by variation in sediment supply.

At a higher hierarchical scale, lobe stacks and lobe sets from the confined and unconfined examples detailed in this study, stack spatially in two distinct ways mainly in response to topographic confinement. In confined lobes, component units pile up vertically (vertical stacking) and compensational processes are unimportant mainly because contained, ponded turbidity currents are not likely to develop lobate, convex upward geometries and lateral shifting of lobe is impeded by basin morphology. As a result, the architecture of confined lobes is sheet-like, with basin-wide extensive lobe stacks shaling and pinch shaling out toward basin margins.

Conversely, in unconfined lobes of Mt. Bilanciere Complex, the depositional architecture is more complicated and shows a combination of vertical and compensational

stacking of lobe stacks and lobe sets. Such architecture can be interpreted as the result of either local compensation of depositional topography or shifting of channel mouths for reorganisation of the channel network in proximal sectors of turbidite systems.

Finally, at the scale of the whole basin-infill, the architecture of the studied interval registers the superimposition of unconfined lobe complexes on top of confined lobe complexes, the rotation of the lobe element axis toward the E and an overall eastward shift of the depocentre as a result of a complex interplay of turbidite sedimentation and thrust propagation.

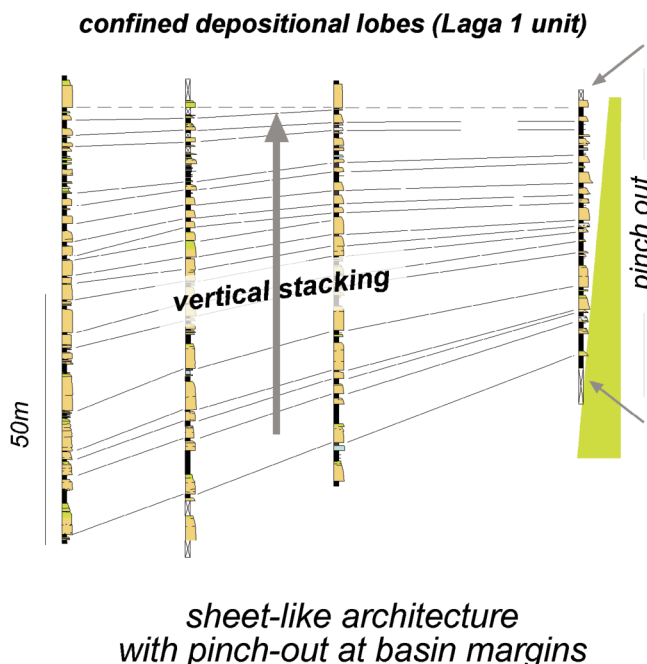
CONCLUSIONS

Depositional processes and architecture of turbidite lobe complexes from the Messinian Laga Basin (Central Apennines, Italy) were greatly controlled by the degree of basin confinement, which in turn was modulated by the interplay of tectonics and turbidite sedimentation. During the Early Messinian, turbidite deposition took place in a dead-end narrow trough bordered by thrust-related anticlines. Progressive filling of the main depocentre of the Southern Laga Basin and tectonic uplift of the more internal sector resulted in a substantial smoothing out of basin morphology and rearrangement of the turbidite systems physiography. From this point onwards, turbidite lobes spilled over the most external, confining anticline to a less confined setting. Such change in basin configuration and degree of topographic confinement gave rise to two distinct lobe depositional architectures for the lower (Laga 1 unit) and upper (Laga 2 unit) part of the studied interval, whose differences are reflected in the whole range of hierarchy, from event beds to lobe complexes.

Due to basin modifications, physical boundary conditions for turbidite deposition changed during the Lower Messinian. In confined lobes of the Laga 1 unit, ponding of turbidity currents and flow blocking by bounding slopes severely controlled flow evolution and depositional processes whilst, in less confined to unconfined lobes of Laga 2 unit turbidity currents were more free to expand outboard from channel mouths. Here, although to a minor degree, depositional microtopography itself was able to force flow transformations and deposition. Besides, in both confined and unconfined settings, seafloor slope resulting from the combination of basin morphology and depositional microtopography sufficed for slumps to initiate and possibly undergo flow transformations.

The case study of the Lower Messinian lobe complexes from the Laga Basin turbidites illustrates how the balance

Depositional architecture of lobe complexes



unconfined depositional lobes (Laga 2 unit)

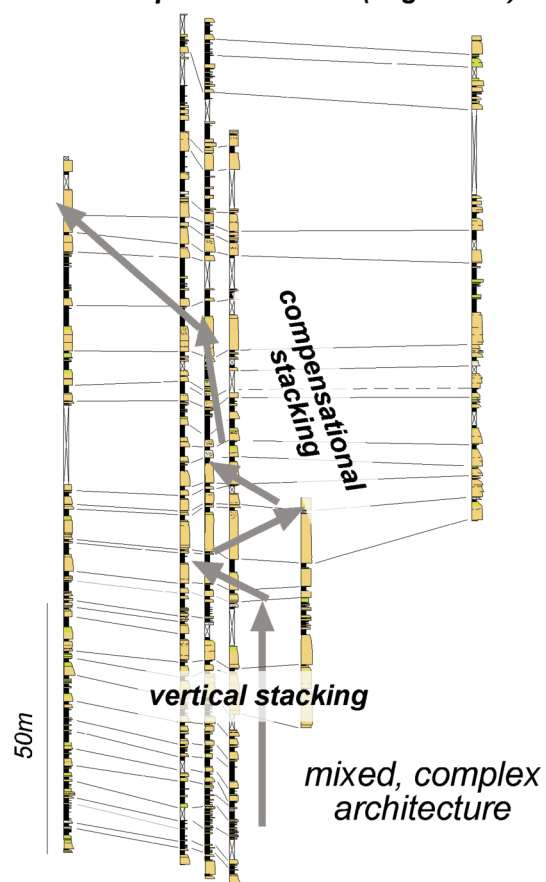


Fig. 25 - The depositional architecture of confined and unconfined lobe complexes.

between growth-rate of intra-basinal highs and turbidite sedimentation may strongly control the degree of basin confinement and, hence, the depositional architecture of turbidite systems. The general validity of such concepts, makes the Laga Basin turbidite succession an excellent depositional analogue for turbidite basins with active tectonics from either alike geodynamic contexts or rifted margins and slopes affected by salt-withdrawal.

ACKNOWLEDGEMENTS - This research beneficiated of the financial support of Norske Shell ASA and Statoil ASA and from thoughtful discussions with Rodmar Ravnas (Norske Shell ASA) and Nicholas Satur (Statoil ASA).

The authors wish to thank Fabrizio Felletti (University of Milano, "A. Desio") and Roberto Tinterri (University of Parma) who reviewed and helped improving the original manuscript, and all colleagues with whom we have had lengthy conversations about turbidites. These include O. Stanzione, G. Gennari, and F. Falcini.

REFERENCES

Alexander J., Morris S. 1994. Observations on experimental, nonchannelized, high-concentration turbidity currents and variations in deposits around obstacles. *Journal of Sedimentary Research*: 64, 899-909.

Al-Ja'aidi O., McCaffrey W.D., Kneller B.C. 2004. Factors influencing the deposit geometry of experimental turbidity currents: implications for sand-body architecture in confined basins, In: Lomas S.A., Joseph P. (Eds.), *Confined Turbidite Systems*. Geological Society, London, Special Publications: 222, 45-58.

Amy L.A., Talling P.J., Edmonds V.O., Sumner E.J., Lesueur A. 2006. An experimental investigation of sand-mud settling behaviour: implications for bimodal mud contents of submarine flow deposits. *Sedimentology*: 53, 1411-1434.

Amy L.A., Kneller B.C., McCaffrey W.D. 2007. Facies architecture of the Gres de Peira Cava, SE France: landward stacking patterns in ponded turbidite basins. *Journal of the Geological Society*: 164, 143-162.

Amy L.A., McCaffrey W.D., Kneller B.C. 2004. The influence of a lateral basin-slope on the depositional patterns of natural and experimental turbidity currents. In: Joseph P., Lomas S.A., (Eds.), *Deep-water sedimentation in the Alpine Basin of SE France: new perspectives on the Grès d'Annot and related systems*. Geological Society, London, Special Publication: 221, 311-330.

Artoni A. 2003. Messinian events within the tectono-stratigraphic evolution of the Southern Laga basin (Central Apennines, Italy). *Bollettino della Società Geologica Italiana*: 122, 447-465.

Artoni A. 2007. Growth rates and two-mode accretion in the outer orogenic wedge-foreland basin system of Central Apennine (Italy). *Bollettino della Società Geologica Italiana*: 126, 531-556.

Ashley G.M. 1990. Classification of large-scale subaqueous bedforms: a new look at an old problem. *Journal of Sedimentary Petrology*: 60, 160-172.

Baas J.H., Best J.L., Peakall J., Wang N. 2009. A phase diagram for turbulent, transitional and lamina clay suspensions flow. *Journal of Sedimentary Research*: 79, 162-183.

Bigi S., Milli S., Corrado S., Casero P., Aldega L., Botti F., Moscatelli M.,

Stanzione O., Falcini F., Marini, M., Cannata D. 2009. Stratigraphy, structural setting and thermal history of the Messinian Laga Basin in the context of Apennine foreland basin system. *Journal of Mediterranean Earth Sciences*: 1, 61-84.

Bigi S., Casero P., Ciotoli G. 2011. Seismic interpretation of the Laga basin; constraints on the structural setting and kinematics of the Central Apennines. *Journal of the Geological Society*: 168, 179-190.

Bouma A.H. 1962. Sedimentology of some flysch deposits, a graphic approach to facies interpretation. Elsevier Co., Amsterdam, 168 pp.

Calamita F., Cello G., Deiana G. 1994. Structural styles, chronology rates of deformation, and time-space relationships in the Umbria-Marche thrust system (Central Apennines, Italy). *Tectonics*: 13, 873-881.

Campbell C.V. 1967. Lamina, laminaset, bed and bedset. *Sedimentology*: 8, 7-26.

Cantalamessa G., Centamore E., Chiocchini U., Di Lorito L., Leonelli M., Micarelli A., Pesaresi A., Potetti M., Taddei L., Venanzini D. 1980. Analisi dell'evoluzione tettonico-sedimentaria dei "bacini minori" torbiditici del Miocene medio-superiore nell'Appennino umbro-marchigiano e laziale-abruzzese: 8) il Bacino della Laga tra il F. Fiastrone - T. Fiastrella ed il T. Fluvione. *Studi Geologici Camerti*: 6, 81-133.

Cantalamessa G., Centamore E., Chiocchini U., Di Lorito L., Micarelli A., Potetti M. 1983. I depositi terrigeni neogenico-quaternari affioranti tra il F. Potenza ed il F. Tronto. *Studi Geologici Camerti*, num. spec., Riunione Gruppo di Sedimentologia del C.N.R., Camerino - S. Benedetto del Tronto, 26-29 Settembre 1983.

Cantalamessa G., Centamore E., Chiocchini U., Micarelli A., Potetti M., con la coll. di Di Lorito L. 1986. Il Miocene delle Marche. *Studi Geol. Camerti*, vol. spec. "La Geologia delle Marche", 35-55.

Carminati E., Doglioni C., Scrocca D. 2004. Alps vs Apennines. In: Crescetti U., D'Offizi S., Merlini S., Sacchi L., (Eds.), *Geology of Italy*. Special Publication of the Italian Geological Society for the IGC 32nd. Florence, 2004, 141-151.

Casnedi R., Ghielmi M., Rossi M., Cazzola L., Serafini G. 2006. Geometrical analysis and seismic modelling of an outer foredeep margin in the Lower Messinian Laga turbidite complex (Centrasl Apennines, Abruzzo, Italy). *Bollettino della Società Geologica Italiana*: 125, 203-220.

Centamore E., Chiocchini U., Cipriani N., Deiana G., Micarelli A. 1978. Analisi dell'evoluzione tettonico-sedimentaria dei "bacini minori" torbiditici del Miocene medio-superiore nell'Appennino umbro-marchigiano e laziale-abruzzese: 5) Risultati degli studi in corso. *Memoria della Società Geologica Italiana*: 18, 135-170.

Centamore, E., Cantalamessa, G., Micarelli, A., Potetti, M., Berti, D., Bigi, S., Morelli, C., and Ridolfi, M. 1991. Stratigrafia e analisi di facies dei depositi del Miocene e del Pliocene inferiore dell'avanfossa marchigiano-abruzzese e delle zone limitrofe. *Studi Geologici Camerti*, vol. spec.: 2, 125-131.

Corda L., Morelli C. 1996. Compositional evolution of the Laga and Cellino sandstones (Messinian-Lower Pliocene, Adriatic foredeep). *Bollettino della Società Geologica Italiana*: 115, 423-437.

Davis C., Haughton P., McCaffrey W., Scott E., Hogg N., Kitching D. 2009. Character and distribution of hybrid sediment gravity flow deposits from the outer Forties Fan, Palaeocene Central North Sea. *UKCS. Marine and Petroleum Geology*: 26, 1919-1939.

Deptuck M.E., Piper D.J.W., Savoie B., Gervais A. 2008. Dimensions and architecture of late Pleistocene submarine lobes off the northern margin of East Corsica. *Sedimentology*: 55, 869-898.

Doglioni C. 1991. A proposal of kynematic modelling for west-dipping subductions - possible application to the Tyrrhenian Apennines system. *Terra Nova*: 3, 423-434.

Falcini F., Marini M., Milli S., Moscatelli M. 2009. An inverse problem to infer paleo-flow conditions from turbidites. *Journal of Geophysical Research*, 114, C10019, doi: 10.1029/2009JC005294.

Gervais A., Savoie B., Mulder T., Gonthie E. 2006. Sandy modern turbidite lobes: a new insight from high resolution seismic data. *Marine and Petroleum Geology*: 485-50.

Ghibaudo G. 1981. Deep-sea fan deposit in the Macigno Formation (middle-upper Oligocene) of the Gordana Valley, northern Apennine, Italy - reply. *Journal of Sedimentary Petrology*: 51, 1021-1033.

Haughton P.D.W., Barker S.P., McCaffrey W. 2003. 'Linked' debrites in sand-rich turbidite systems - origin and significance. *Sedimentology*: 50, 459-482.

Haughton P., Davis C., McCaffrey W., Barker S. 2009. Hybrid sediment gravity flow deposits - classification, origin and significance. *Marine and Petroleum Geology*: 26, 1900-1918.

Hiscott R.N. 1981. Deep sea fan deposits in the Macigno Fm. (Middle-Upper Oligocene) of the Gordana Valley, Northern Apennines, Italy: Discussion. *Journal of Sedimentary Petrology*: 51, 1015-1021.

Kneller B.C. 1995. Beyond the turbidite paradigm: physical models for deposition of turbidites and their implications for reservoir prediction. In: Hartley A.J., Prosser D.J. (Eds.), *Characterization of Deep Marine Clastic Systems*. Geological Society, London, Special Publication: 94, 31-49.

Kneller B.C., Edwards D.A., McCaffrey W.D., Moore R. 1991. Oblique reflection of turbidity currents. *Geology*: 19, 250-252.

Kneller B.C., Bennet S.J., McCaffrey W.D. 1997. Velocity and turbulence structure of gravity currents and internal solitary waves: potential sediment transport and the formation of wave ripples in deep waters. *Sedimentary Geology*: 112, 235-250.

Kneller B.C., Branney M.J. 1995. Sustained high-density turbidity currents and the deposition of thick massive sands. *Sedimentology*: 42, 607-616.

Kneller B.C., McCaffrey W.D. 1999. Depositional effects of flow nonuniformity and stratification within turbidity currents approaching a bounding slope; deflection, reflection, and facies variation. *Journal of Sedimentary Research*: 69, 980-991.

Lowe D.R. 1975. Water escape structures in coarse-grained sediments. *Sedimentology*: 22, 157-204.

Lowe D.R. 1982. Sediment gravity flows: II depositional models with special reference to the deposits of high-density turbidity current. *Journal of Sedimentary Petrology*: 52, 279-297.

Lowe D.R., Guy M. 2000. Slurry flow deposits in the Britannia Fm. (Lower Cretaceous), North Sea: a new perspective on the turbidity current and debris flow problem. *Sedimentology*: 47, 31-70.

Lowe D.R., Guy M., Palfrey A. 2003. Facies of slurry-flow deposits, Britannia Fm. (lower Cretaceous), North Sea: implications for flow evolution and deposit geometry. *Sedimentology*: 50, 45-80.

Lüthi S. 1981. Some new aspects of two-dimensional turbidity currents. *Sedimentology*: 28, 97-105.

Marini M., Milli S., Moscatelli M. 2009. Facies and geometries of turbidite lobe deposits from the Messinian Laga Fm. (central Apennine, Italy). In: Pascucci V., Andreucci S. (Eds.), *Abstract Book. 27th IAS Meeting of Sedimentology Alghero, September 20-23, 2009, Sassari (Italy)*, 264.

Marini M. 2010. Architecture of turbidite lobe complexes from the Messinian Laga Basin (central Apennines, Italy). Ph.D. Thesis, Università di Roma "La Sapienza", 123 pp.

Manzi V., Lugli S., Ricci Lucchi F., Roveri M. 2005. Deep-water clastic evaporites deposition in the Messinian Adriatic foredeep (Northern Apennines, Italy): did the Mediterranean ever dry out? *Sedimentology*: 52, 875-902.

Milli S., Moscatelli M., Stanzione O., Falcini F. 2007. Sedimentology and physical stratigraphy of the Messinian turbidite deposits of the Laga basin (central Apennines, Italy). *Bollettino della Società Geologica Italiana*: 126, 255-281.

Milli, S., Moscatelli, M., Marini, M., and Stanzione, O. 2009. The Messinian turbidite deposits of the Laga basin (central Apennines, Italy) In: Pascucci V., Andreucci S. (Eds.), *Field Trip Guide Book, Post-conference trip FT12, 27th IAS Meeting of Sedimentology Alghero, September 20-23, 2009*: 279-297.

Morelli C. 1994. Ricostruzione dell'evoluzione tettonico-sedimentaria dei bacini di avanfossa Marchigiano-Abruzzesi durante il Messiniano-Pliocene Inferiore. Ph.D. Thesis, Università di Roma "La Sapienza", 170 pp.

Mutti E. 1977. Distinctive thin-bedded turbidite facies and related depositional environments in the Eocene Hecho Group (South-

Central Pyrenees, Spain). *Sedimentology*: 24, 107-131.

Mutti E. 1979. Turbidites et cones sous-marine profonds. In: Homewood P. (Ed.), *Sedimentation detritique (fluviaatile, littorale e marine)*. Istitut de Geologia, Université de Fribourg, Fribourg, 353-419.

Mutti E. 1992. Turbidite sandstones. Agip, Istituto di Geologia, Università di Parma, San Donato Milanese, 275 pp.

Mutti E., Ghibaudo G. 1972. Un esempio di torbiditi di conoide esterna: le Arenarie di San Salvatore (Formazione di Bobbio, Miocene) nell'Appennino di Piacenza. *Memorie dell'Accademia delle Scienze di Torino, Classe Scienze Fisiche Matematiche Naturali*: 16, 1-40.

Mutti E., Nilsen T.H., Ricci Lucchi F. 1978. Outer fan depositional lobes of Laga Fm. (Upper Miocene and Lower Pliocene), east central Italy. In: Stanley D.J., Kelling G. (Eds.), *Sedimentation in submarine canyons, fans and trenches*. Downed, Hutchinson & Ross, 210-223.

Mutti E., Normark W.R. 1987. Comparing examples of modern and ancient turbidite systems: problems and concept. In: Legget J.K., Zuffa G.G. (Eds.), *Marine clastic sedimentology*, Springer, New York, 1-38.

Mutti E., Normark W.R. 1991. An integrated approach to the study of turbidite systems. In: Weimer P., Link H. (Eds.), *Seismic facies and sedimentary processes of submarine fans and turbidite systems*. Springer-Verlag, 75-106.

Mutti E., Ricci Lucchi F. 1972. Le torbiditi dell'Appennino settentrionale: introduzione all'analisi di facies. *Memorie della Società Geologica Italiana*: 1, 161-199.

Mutti E., Ricci Lucchi F. 1975. Turbidite facies and facies association. In: Mutti E., Parea G.C., Ricci Lucchi F., Sagri M., Zanzucchi G., Ghibaudo G., Iaccarino S. (Eds.), *Examples of turbidite facies associations from selected Fm. of Northern Apennines*. IX International Congress IAS, Field Trip, All., Nizza, 21-36.

Mutti E., Sonnino M. 1981. Compensation cycles: a diagnostic feature of sandstone lobes. International Association of Sedimentologists, 2nd European Meeting, Bologna, abstracts volume, 120-123.

Mutti E., Tinterri R., Remacha E., Mavilla N., Angella S., Fava L. 1999. An introduction to the analysis of ancient turbidite basins from an outcrop perspective. AAPG Continuing Education Course Note Series 39, 61 pp.

Muzzi Magalhaes P., Tinterri R. 2010. Stratigraphy and depositional setting of slurry and contained (reflected) beds in the Marnoso-arenacea Fm. (Langhian-Serravallian) Northern Apennines, Italy. *Sedimentology*: 57, 1685-1720.

Pantin H.M., Leeder M.R. 1987. Reverse flow in turbidity currents; the role of internal solitons. *Sedimentology*: 34, 1143-1155.

Patacca E., Sartori R., Scandone P. 1990. Tyrrhenian basin and apenninic arcs: kinematic relations since late Tortonian times. *Memorie della Società Geologica Italiana*: 45, 425-451.

Pickering K., Stow D.A.V., Watson M., Hiscott R. 1986. Deep water facies, processes and models: a review and classification scheme for modern and ancient sediments. *Earth Science Reviews*: 23, 75-174.

Postma G. 1986. Classification for sediment gravity-flow deposits based on flow conditions during sedimentation. *Geology*: 14, 291-294.

Remacha E., Fernández L.P., Maestro E. 2005. The transition between sheet-like lobe and basin-plain turbidites in the Hecho Basin (South-Central Pyrenees, Spain). *Journal of Sedimentary Research*: 75, 798-819.

Ricci Lucchi F. 1978. Turbidite dispersal in a Miocene deep sea plain. *Geol. Mijnbouw*: 57, 559-576.

Ricci Lucchi F. 1981. The Marnoso-arenacea turbidites, Romagna and Umbria Apennines. In: Ricci Lucchi F. (Ed.), *Excursion Guidebook with contribution on sedimentology of some Italian basins*. IAS 2nd European Regional Meeting Bologna, 229-303.

Ricci Lucchi F. 1986. The Oligocene to recent foreland basin of the Northern Apennines. In: Allen P.A., Homewood P., (Eds.), *Foreland basins*. IAS Special Publication: 8, 105-139.

Ricci Lucchi F., Valmori E. 1980. Basin-wide turbidites in Miocene, over-supplied deep-sea plain: a geometrical analysis. *Sedimentology*: 27, 241-270.

Rossi M., Rogledi S., Barbacini G., Casadei D., Iaccarino S., Papani G. 2002. Tectono-stratigraphic architecture of Messinian piggyback basins of Northern Apennines: the Emilia folds in the Reggio-Modena area and comparison with the Lombardia and Romagna sectors. *Bollettino della Società Geologica Italiana*: volume speciale 1, 437-447.

Roveri M., Manzi V., Bassetti M.A., Merini M., Ricci Lucchi F. 1998. Stratigraphy of the Messinian post-evaporitic stage in eastern-Romagna (Northern Apennines, Italy). *Giornale di Geologia*: 60, 119-142.

Sanders J.E. 1965. Primary sedimentary structures formed by turbiditic currents and related resedimentation mechanisms. In: Middleton, G.V. (Ed.), *Primary sedimentary structures and their hydrodynamic interpretation*. SEPM (Society for Sedimentary Geology) Special Publication: 12, 192-219.

Satur N., Hurst A., Cronin B.T., Kelling G., Gürbüz K. 2000. Sand body geometry in a sand-rich, deep-water clastic system, Miocene Cingöz Fm. of southern Turkey. *Marine and Petroleum Geology*: 17, 239-252.

Sinclair H.D. 1994. The influence of lateral basinal slopes on turbidite sedimentation in the Annot sandstones of SE France. *Journal of Sedimentary Research*: 64a, 42-54.

Sylvester Z., Lowe D.R. 2004. Textural trends in turbidites and slurry beds from the Oligocene flysch of the East Carpathians, Romania. *Sedimentology*: 51, 945-972.

Talling P.J., Amy L.A., Wynn R.B., Peakall J., Robinson M. 2004. Beds comprising debrite sandwiched within co-genetic turbidite: origin and widespread occurrence in distal depositional environments. *Sedimentology*: 51, 163-194.

Watterson J., Walsh J., Nicol A., Nell P.A.R., Bretan P.G. 2000. Geometry and origin of a polygonal fault system. *Journal of the Geological Society*: 157, 151-162.